Published in final edited form as:
Biochim Biophys Acta. 2008 September ; 1777(9): 1079–1091. doi:10.1016/j.bbabio.2008.04.022.

Regulatory interactions in the dimeric cytochrome bc_1 complex: The advantages of being a twin

Raul Covian and **Bernard L. Trumpower**[a]
Department of Biochemistry, Dartmouth Medical School Hanover, New Hampshire 03755, U.S.A.

Abstract

The dimeric cytochrome bc_1 complex catalyzes the oxidation-reduction of quinol and quinone at sites located in opposite sides of the membrane in which it resides. We review the kinetics of electron transfer and inhibitor binding that reveal functional interactions between the quinol oxidation site at center P and quinone reduction site at center N in opposite monomers in conjunction with electron equilibration between the cytochrome *b* subunits of the dimer. A model for the mechanism of the bc_1 complex has emerged from these studies in which binding of ligands that mimic semiquinone at center N regulates half-of-the-sites reactivity at center P and binding of ligands that mimic catalytically competent binding of ubiquinol at center P regulates half-of-the-sites reactivity at center N. An additional feature of this model is that inhibition of quinol oxidation at the quinone reduction site is avoided by allowing catalysis in only one monomer at a time, which maximizes the number of redox acceptor centers available in cytochrome *b* for electrons coming from quinol oxidation reactions at center P and minimizes the leakage of electrons that would result in the generation of damaging oxygen radicals.

Keywords

bc_1 complex; Electron transfer; Quinone; Stigmatellin; Antimycin

1. Introduction

The cytochrome bc_1 complex is present in the inner membrane of most mitochondria and heterotrophic bacteria. The functional core of this respiratory enzyme is comprised of the highly hydrophobic diheme cytochrome *b* associated with the trans-membrane regions of the Rieske iron-sulfur protein and cytochrome c_1. One of the most surprising features revealed by the atomic-resolution structures of the bc_1 complex [1–5] is that this enzyme can only function as a dimer (Fig. 1). The inclination of the trans-membrane helix of the Rieske protein results in the interaction of its extramembrane domain with the quinol oxidation site (center P) of cytochrome *b* in the opposite monomer.

In the protonmotive Q cycle mechanism [6, reviewed in Ref. 7], one of the two electrons coming from the oxidation of quinol at center P, located close to the positive side of the membrane, is transferred to cytochrome *c* via the Rieske protein and cytochrome c_1. The other electron from

aTo whom correspondence should be addressed: Department of Biochemistry, Dartmouth Medical School, 7200 Vail, Hanover, NH 03755. Phone: 603-650-1621; Fax: 603-650-1128; E-mail: Trumpower@Dartmouth.edu.

quinol moves from the b_L to the b_H heme across the membrane dielectric and reduces quinone bound at center N to form a stable, tightly bound semiquinone [8–10]. A further quinol oxidation event at center P donates the electron needed to reduce semiquinone to quinol at center N. The deprotonation of quinol at center P and the protonation of quinone at center N results in the net movement of protons across the membrane, which together with the movement of the negative charge of the electron from b_L to b_H, contributes to the formation of a protonmotive gradient.

Having two sites catalyzing the same net reaction in opposite directions (oxido-reduction of quinol/quinone) introduces the potential for significant inhibition of quinol oxidation at center P by the reversibility of reactions at center N. The lack of oxidized acceptors in cytochrome *b* for the second electron coming from center P would result in detrimental reactions, such as the one electron reduction of oxygen to form superoxide [11]. Therefore, mechanisms that avoid the accumulation of electrons in cytochrome *b* are expected to exist in the bc_1 complex. In this article, we review the experimental evidence showing how the dimeric structure of the bc_1 complex allows the regulation of center P and center N in a manner that maximizes the availability of electron acceptors in cytochrome *b* in order to avoid electron leakage out of center P.

2. Half-of-the-sites activity at center P

2.1 Inactivation of one center P in the presence of antimycin

One possible mechanism that can be envisioned in order to decrease spurious electron transfer to oxygen in a dimeric bc_1 complex is to avoid simultaneous quinol oxidation at both center P sites. Evidence for the existence of this mechanism was first provided in pre-steady state assays in which the semi-purified bovine complex was reduced with duroquinone, a more hydrophilic analog of ubiquinone [12]. It was reported that with antimycin bound at both center N sites only half of the iron-sulfur clusters and of the c_1 hemes were reduced in a fast phase, while the remaining fraction underwent reduction much more slowly, possibly by the one-electron oxidation of duroquinol that accompanies superoxide formation at center P [11]. However, this result was interpreted as indicating that antimycin could bind directly to one quinol oxidation site in the dimer [12], which has been disproved by the structural information now available [13].

It has also been claimed [14] that the incomplete reduction of the Rieske protein and of cytochrome c_1 in the presence of antimycin (which blocks the oxidation of the b_H heme through center N) is simply a consequence of only one quinol oxidation event occurring in every center P. Since a second quinol oxidation would imply the reduction of heme b_L (which has a redox potential 120–150 mV lower than that of b_H), this interpretation assumes that the less favorable equilibrium constant for a second turnover when the b_H heme is already reduced would allow only one electron coming from the first catalysis at each center P to reside in either the Rieske protein and cytochrome c_1.

We have excluded the “one turnover per monomer” explanation for the missing cytochrome c_1 reduction in the presence of antimycin [14] by using conditions in which even a single quinol oxidation event should result in an electron residing preferentially in cytochrome c_1 [15]. This was accomplished with the yeast bc_1 complex by using alkaline conditions to decrease the pH-dependent redox potential of the Rieske protein, or by mutation of one of the residues that controls the redox potential of the iron-sulfur cluster. As shown in Fig. 2 where data from Ref. 15 is reproduced, both at pH 8.8 with the wild-type yeast enzyme (Fig. 2A), or at neutral pH with the Y185F Rieske mutant (Fig. 2B), cytochrome c_1 reduction (corrected for the contribution of the b_H heme at the measured wavelengths) stays below 50% in the presence of antimycin (red traces). In both cases, the redox potential of the Rieske protein is 60–70 mV

lower than cytochrome c_1, resulting in an expected reduction of ~80% of the c_1 heme, assuming every center P catalyzed one quinol oxidation reaction. This was approximately the reduction level attained in the uninhibited enzyme (blue traces in Fig. 2), indicating that both center P sites in the dimer are able to react when center N is free to recycle electrons.

Since quinol can reduce the b_H heme directly by binding to center N in a reaction faster than that through center P, cytochrome c_1 reduction did not reach 100% in the absence of antimycin due to the amount of pre-reduced b_H present before the first turnover at center P. However, in the presence of the center N inhibitor (red traces in Fig. 2), the observed reduction level in c_1 could be accurately explained by assuming that one turnover occurred only at half of the center P sites (solid black line), but not in both monomers (dashed line). Simulations that included the calculated equilibrium constants for quinol oxidation in the presence of antimycin [15] showed that a second turnover (Keq ~1) was possible under the conditions used, explaining the further reduction of c_1 from 40% to 50% (red traces in Fig. 2). We also demonstrated that in the presence of several equivalents of oxidized cytochrome *c*, which further favor a second turnover at the active center P, only two turnovers per dimer occur when antimycin is bound to the enzyme, again indicating that one center P per dimer was inactive [15]. The well-known phenomenon of oxidant-induced reduction of at least part of the b_L hemes in the presence of antimycin, shown both in bacterial [16] and mitochondrial enzymes [17], indicates that further turnovers at the active center P site are possible even when the b_H hemes are reduced, as long as cytochrome *c* is present and maintained oxidized, and enough quinol is available. Under such conditions, a single active center P site per dimer could reduce any of the two b_L hemes provided that there is electron communication between them. Evidence for inter-monomeric electron transfer is discussed below (Section 4).

Similar results to those shown in Fig. 2 were obtained with the *Paracoccus denitrificans* bc_1 complex [18], indicating that this half-of-the-sites activity is not exclusive to yeast, but is a conserved feature even in the simpler bc_1 complexes from bacteria, which are devoid of the non-redox subunits present in the eukaryotic complexes. The bacterial enzyme has mostly been studied in chromatophore membranes of *Rhodobacter* [19,20], in which the bc_1 complex is present together with the endogenous ubiquinone pool (which is usually poised at a particular redox potential with artificial mediators) and the diffusible cytochrome c_2 (equivalent to the soluble cytochrome *c* of mitochondria). However, little attention has been given in these studies as to the reasons that could account for the incomplete reduction of the *c*-type cytochromes in the presence of antimycin, which is ~30% of the extent observed in the uninhibited condition at neutral pH [14], except for the “one turnover per monomer” argument discussed above.

Nevertheless, a dimeric alternating mechanism for quinol oxidation at center P has been proposed for the bacterial bc_1 complex in chromatophores [21]. This model proposed that the oxidation of one quinol molecule per dimer could only be driven by the thermodynamically more favorable catalysis at center P in the other monomer, and that the presence of either semiquinone or quinol at center N could determine whether quinol oxidation at each center P could occur. However, this proposal assumed that absolutely no ubiquinol could be formed by the bacterial reaction center upon a single, low intensity flash, and that one ubiquinol molecule per dimer stayed reduced for several seconds even at an oxidizing redox potential of 250 mV in the presence of redox mediators (implying that it remained tightly bound to center P), even though it was readily oxidized upon activation of the reaction center by the weak flash [21]. In addition, the equilibrium constants for center P turnovers were assumed to be determined by the redox potential of the semiquinone or quinone molecules bound at center N, and not by the potential of the b_H heme, which is the actual electron acceptor. The experimental support for this model was thus questionable at the time it was proposed, although some of its postulates, such as an alternating site mechanism for center P, the existence of electron exchange between

two monomers, and the conformational coupling between centers P and N, have been confirmed by more recent studies, as discussed in this review.

The complexity of the chromatophore system, where reaction centers form ternary complexes with an undetermined fraction of the bc_1 complexes in the chromatophore membrane to reduce ubiquinone and simultaneously oxidize the *c*-type cytochromes to generate ubiquinol in the pool, increases the difficulty in interpreting kinetic data in terms of a dimeric mechanism. In contrast, the simpler assays in which the isolated bc_1 complex is mixed with known concentrations of substrates and products have led to more straightforward conclusions involving the functional relevance of the dimer [15,18]. The solubilized enzyme system also allows working below the K_m values for quinol simply by increasing the detergent concentration. This results in lower reaction rates that are amenable to the collection of complete spectra every millisecond. The under-saturation of the enzyme with respect to its substrate does not change the rate limiting step, since center P catalysis is still controlled by the midpoint potential of the Rieske protein [22], as has also been observed in chromatophores [23]. Moreover, the reliability of the isolated enzyme system is illustrated, for example, by the linear Arrhenius plots for the determination of activation energies that are obtained with this experimental setup [24], but not with the chromatophore system [25].

2.2 Asymmetric binding of inhibitors to center P: Evidence of anti-cooperative quinol oxidation

The inactivation of quinol oxidation at one center P per dimer when ligand is bound at center N in both monomers suggests that the interaction of the extrinsic domain of the Rieske protein with the surface of cytochrome *b* is altered, preventing the formation of the enzyme-substrate complex. This productive configuration is thought to resemble the conformation observed in crystal structures when stigmatellin is bound to center P [1,4]. This inhibitor forms a hydrogen bond to one of the histidine residues that ligates the iron-sulfur center, and this same interaction is thought to exist between quinol and the Rieske protein in order for electron transfer to occur. Tight binding of stigmatellin requires the presence of the Rieske protein in the bc_1 complex [26], and its binding site shows significant changes depending on the position of the Rieske extrinsic domain [27]. Therefore, if the bc_1 complex dimer functions by allowing only one center P to be active at a time, stigmatellin should bind differently to each center P in the dimer.

This is precisely what we have found by analyzing the binding of stigmatellin to the *P. denitrificans* bc_1 complex, which exhibits a significant blue shift of the b_L heme absorbance peak upon binding of this inhibitor [18]. As shown in Fig. 3, stigmatellin binds to one half of the center P sites more rapidly than to the other, generating in the end an asymmetric shift on the b_L spectrum, which indicates a different configuration of the inhibitor in half of the sites. Deconvolution of the spectral shift produced by each kinetic binding phase showed that the initial faster binding event generated a symmetric shift, while the slower binding resulted in a change in the shape of the b_L spectrum, indicating a slightly different position of the inhibitor in each center P [18]. In addition, the rate of the slow phase of stigmatellin binding was shown to be independent of inhibitor concentration, which suggests a sequential binding process that requires a slow conformational change after the initial binding to the first half of the center P sites. The difference in the rate of the two phases increased, while the extent of the slower phase decreased, at higher stigmatellin concentrations [18], indicating that heterogeneity in the enzyme sample (which also exhibited full cytochrome c_1 reduction activity) was not responsible for the biphasic binding of the inhibitor. We have interpreted the progressive loss in the extent of the slow phase of stigmatellin binding to the ability of the inhibitor at higher concentrations to bind to the second monomer before a conformational change induced by binding to the first monomer modifies the second center P site [18]. Therefore, these results support the conclusion that one center P in the dimer is impeded at least partially from acquiring

the catalytically competent configuration in which the Rieske protein is able to accept electrons from quinol. This might be achieved not only by an effect on the position of the extrinsic domain of the Rieske protein in the second monomer, but also by any change that decreases the affinity toward quinol in the second center P. Either of these mechanisms, or a combination of both, would result in the observed anti-cooperative oxidation of quinol.

Additional evidence supporting a half-of-the-sites activity at center P was obtained by titrating the steady-state activity of quinol oxidation with inhibitors that are sensitive to the position of the extrinsic domain of the Rieske protein [28]. It was found that only one molecule per dimer of stigmatellin or MOA-stilbene was sufficient for complete inhibition of quinol oxidation, indicating that only one center P was active and in the correct conformation to allow efficient binding of these inhibitors. The rate constant for stigmatellin binding has been found to be higher when the Rieske protein is reduced, even though its binding to center P is still tight when the enzyme is fully oxidized [29]. The binding of MOA-stilbene is also sensitive to the redox state of the Rieske protein [30], indicating that the position of the extrinsic domain of the Rieske protein, which influences the redox potential of iron-sulfur cluster [31,32], modifies the affinity for these two inhibitors.

In contrast, myxothiazol, the binding of which is largely insensitive to the position of the Rieske protein [30], was apparently able to bind to both active and inactive center P sites, given that two molecules per dimer were needed to completely block the activity [28]. In agreement with this result, we observed that myxothiazol binds with a single rate to all center P sites of the *P. denitrificans* bc_1 complex, generating a symmetrical spectral shift of the b_L heme [18]. This homogeneous binding of myxothiazol obviates the possibility of heterogeneity in the enzyme preparation. Nevertheless, under some circumstances even myxothiazol seems to bind preferentially to one monomer, as observed in a mutant yeast bc_1 complex in which the Rieske protein lacks the iron-sulfur center [33].

3. Interaction between center P and center N sites in the dimer

3.1 Asymmetric binding of antimycin to center N

The above mentioned observation that one quinol oxidation site in the dimer is inactivated in the presence of antimycin, but not in its absence (see Fig. 2), implies conformational communication between center P and center N. A number of observations agree with this assumption, including the increased mobility of the Rieske extrinsic domain in the presence of antimycin as measured by its susceptibility to proteolysis [34], as well as the modified interaction of the Rieske protein with center P ligands by center N mutations [35]. In line with this evidence, we found that the binding kinetics of antimycin to center N measured by the red shift generated in the b_H spectrum is affected by center P ligands [36]. As shown in Fig. 4A, where data from Ref. 36 is reproduced, the binding of antimycin when center P is occupied by myxothiazol is monophasic, and its rate is concentration-dependent (Fig. 4C), which indicates that the binding is homogeneous and limited by the diffusion of the inhibitor into center N. This experiment obviates the possibility of a heterogeneous mixture of damaged and intact enzyme. Identical results were obtained in the absence of center P inhibitors [36].

However, when stigmatellin occupies center P, antimycin binding to half of the center N sites is slower and concentration-independent (Fig. 4B, D, taken from Ref. 36), which indicates that one monomer cannot bind the inhibitor until binding to the first center N site induces a relatively slow conformational change that enables binding to the second monomer. Since stigmatellin (but not myxothiazol) fixes the position of the Rieske protein to the proximity of center P [27, 37], our conclusion from these studies is that when both center P sites in the dimer are in the catalytically competent conformation, only one center N is able to bind ligands effectively. Perhaps related to this interpretation, we have found that a mutation that prevents the insertion

of the iron-sulfur cluster into the Rieske cluster also results in the binding of antimycin to only half of the center N sites [33].

A further relevant result from the antimycin binding studies [36] was that quinol did not slow the binding of the inhibitor, indicating that antimycin and quinol bind to different conformations of center N. This suggests that antimycin, which is a tightly bound ligand ($K_d < 10^{-9}$ M [38]), mimics the stable semiquinone intermediate found at this site. Although it has long been known that semiquinone formation at center N is impeded by antimycin [8–10], it has more recently been proposed that this inhibitor mimics quinol [35]. However, the most straightforward way to interpret the insensitivity of antimycin binding rate with respect to the increase in quinol concentration is that these two center N ligands do not compete with each other for the same conformation of center N. Moreover, antimycin binds tightly to center N irrespective of the redox state of the b_H heme, as judged by its lack of effect on the midpoint potential of the heme [39], just as semiquinone is expected to do. This is consistent with an early proposal [40] that antimycin mimics the stable semiquinone intermediate. Therefore, it can be assumed that oxidation of quinol occurs at only one center P when semiquinone is occupying both center N sites, as observed when antimycin is bound to both monomers (see Fig. 2). In turn, the rapid binding of antimycin to only one center N when both center P sites are fixed by stigmatellin in a conformation that resembles the active state (Fig. 4B) implies that whenever semiquinone is stabilized at only one center N site, both center P sites become catalytically competent for quinol oxidation. Experimental evidence supporting these assumptions is discussed in more detail below.

3.2 Half-of-the-sites activity at center N

The physiological relevance of the antimycin binding results was tested by analyzing the kinetics of cytochrome *b* reduction through center N when center P was inhibited by stigmatellin or myxothiazol [36,41]. Under these conditions, quinol binds to center N, followed by the formation of a stable semiquinone upon the one electron reduction of the b_H heme [42,43]. The kinetic traces in Fig. 5, reproduced from Ref. 41, show that the pattern of b_H reduction is sensitive to the type of center P inhibitor present, confirming the existence of a communication pathway between center P and center N. In the presence of stigmatellin, the reduction kinetics include a slow reoxidation phase not observed with myxothiazol. Also, the extent of b_H reduction remained higher with stigmatellin blocking center P than with myxothiazol. Interestingly, in both conditions quinone was unable to fully oxidize cytochrome *b*, and did not affect the initial rate of reduction by quinol, indicating a lack of competition between the two substrates of center N [41]. We also showed that, after equilibration, the EPR properties of semiquinone at center N in the presence of myxothiazol or stigmatellin were the same as in the uninhibited enzyme, indicating that the center P inhibitors were not exerting any significant changes in the redox potential of the tightly bound radical or the b_H heme [41]. In agreement with this observation, it has been shown in different bc_1 complexes that stigmatellin and myxothiazol induce negligible changes in the midpoint potential of the b_H heme [39,44].

We were able to model the fairly complicated kinetic pattern of b_H reduction through center N [41] by assuming the three conditions illustrated in Fig. 6. First, quinol binds to center N preferentially when the b_H heme is oxidized, and quinone when the heme is reduced (intermediates I, III and III'). Second, one center N in the dimer is not able to stabilize semiquinone (intermediate I) until the other center N site has done so (reaction 1 leading to intermediate II). The differences in the kinetics of b_H reduction through center N in the presence of different center P inhibitors can be explained by assuming that stigmatellin bound at the center P sites significantly slows down the activation of the second center N site. Third, electrons are able to equilibrate between the two center N sites in the dimer. Although the evidence for this last assumption is more fully explained in the next section, it is clear from

the model in Fig. 6 that quinone would not be able to decrease the extent of b_H reduction (reaction 3' leading to intermediate IV') unless the electron from the first center N (where semiquinone is now tightly bound) is able to reduce the oxidized b_H heme in the other monomer, allowing the binding of quinone (reaction 2' leading to intermediate III'). Electron equilibration between monomers also explains why b_H oxidation even at high quinone concentrations is only partial (see Fig. 5), yielding a mixed population of intermediates III and III'. Whenever the electron is still residing in the b_H heme of the first center N (intermediate III), quinol will be able to bind to the second center N and reduce its b_H heme (reaction 3 leading to intermediate IV).

The mechanism of half-of-the-sites activity at center N presented in Fig. 6 allows for the existence of at least a fraction of the bc_1 complex dimers with two semiquinones, each one next to an oxidized b_H heme [41,45]. This configuration, with cytochrome *b* fully oxidized and insulated from reduction by reverse quinol oxidation at center N, is optimal for unimpeded center P catalysis, and could not exist at significant concentrations when quinol/quinone ratios are high unless the three conditions outlined above are met. It is true that the conditions in which center N functions by itself while center P is completely blocked are rarely to be found physiologically (see Fig. 5). However, the fact that quinol oxidation at center P is significantly slower than the reversible reactions at center N indicates that all the reactions shown in Fig. 6 have enough time to occur between catalytic turnovers at center P. Therefore, a half-of-the sites mechanism at center N allows cytochrome *b* to be poised in the right redox state to receive the electron from the next quinol oxidation event at center P.

Recently, a dimeric mechanism for the bacterial bc_1 complex was proposed that assumes that only one semiquinone per dimer can be formed [20], an idea already featured in a much earlier proposal [12]. The alleged basis for this model is the observation that no more than ~0.5 semiquinone equivalents per bc_1 monomer are detected by EPR in redox titrations [8–10,39, 41], even after correcting for the antiferromagnetic silencing of the EPR signal when the b_H heme is oxidized [46]. However, as acknowledged by the authors of that dimeric model [20], the electron in the semiquinone formed in one monomer must be in equilibrium with the oxidized b_H heme in its vicinity given the midpoint potentials of the heme and of the redox couples involved in semiquinone formation. When these potentials are considered, it has been shown by simulations that the 0.5 equivalents of semiquinone observed per dimer are simply the result of the probability of the electron residing in semiquinone or in the b_H heme at a given time [39]. We have also simulated semiquinone equilibration at both monomers, suggesting that a mixture of dimers with zero, one or two semiquinones could account for an average of <0.5 equivalents per center N site depending on the quinol/quinone ratio [41]. The only condition in which one center N in the dimer exhibits a lower ligand occupancy is in the presence of stigmatellin, as reported for the yeast bc_1 complex crystallized with cytochrome *c* [47]. In the uninhibited enzyme, other crystal structures have shown ubiquinone bound at both center N sites [13,48], implying that semiquinone could potentially be formed in both monomers. The antimycin binding results we have discussed above (see Section 3.1) also support the notion that ligands such as semiquinone can be rapidly stabilized at both center N sites, except for the condition in which the Rieske protein is fixed close to center P in both monomers (as occurs in the presence of stigmatellin), where tight binding to one center N is impaired at least temporarily.

3.3 Possible routes for conformational communication in the dimer

The wealth of structural information available from crystallographic studies of the bc_1 complex [1–5,13,27,47,48] can be examined in an attempt to identify regions of cytochrome *b* that might be involved in transmitting conformational changes from center P and center N within each monomer and across the dimer. Large-scale differences in center P or center N when an

inhibitor is bound at the other site are not observed, indicating either subtle or short-lived conformational changes. Nevertheless, it has been carefully documented how center P inhibitors significantly modify the surface of cytochrome *b* where the extrinsic domain of the Rieske protein docks in order to catalyze quinol oxidation [27]. This region of the protein includes the CD and EF loops and helices, which are connected to center N residues through the D and E trans-membrane helices. In this regard, a change in rigidity of the D helix has been suggested upon binding of antimycin, which produces subtle changes in the EPR spectrum of the b_L heme in a bacterial bc_1 complex [35]. We have also reported that reverse quinol oxidation at center N can be perturbed by some center P mutations [49]. Still, the exact mapping of the communication pathway between center P and center N within the same monomer awaits further mutational studies.

Structural asymmetries between monomers are impossible to see in most crystal structures simply because they have a monomer in the asymmetric unit [50], resulting in the averaging out of any differences between monomers. The few structures that have a dimer in the asymmetric unit have revealed potentially interesting differences between monomers. In the bovine bc_1 complex dimer [3], it has been revealed that in one monomer the Rieske extrinsic domain is relatively static in an intermediate position between the interfaces with cytochrome *b* and cytochrome c_1, while in the other monomer the Rieske domain is highly movable as indicated by its high degree of disorder. The yeast bc_1 complex crystallized in the presence of cytochrome *c* and stigmatellin [47] has shown a significantly different quinone occupancy at the two center N sites while cytochrome *c* is bound to only one monomer. We have proposed that center P in one monomer could be influenced by center N in the other monomer through the trans-membrane region of the Rieske protein, which traverses the dimer, given that some residues from the Rieske trans-membrane region are in contact with cytochrome *b* residues of helix E on the side facing away from center N [33]. However, residues from the trans-membrane region of cytochrome c_1 are wedged between the Rieske protein and center N in the vertebrate and bacterial enzymes [1–3], implying a lack of conservation in this region.

It seems more likely that center P and center N communicate within each monomer, and that the inter-monomeric conformational changes are transmitted at the level of the center N sites through the amino-terminal region of each cytochrome *b* [36]. Fig. 7 illustrates how the helical region between Tyr-9 and Ile-17 of the yeast cytochrome *b* extends parallel to the plane of the membrane to make contact with Met-196, Met-199 and Ala-200 of the opposite monomer. These residues are close to His-202, which is one of the key residues for binding and catalysis at center N [4,51,52]. This helix is in contact with His-202 in its own monomer through Tyr-16, thus establishing a potential communication pathway between His-202 of both monomers. The interaction pattern of this helix is similar in other bc_1 complexes, but with different residues occupying the corresponding positions; Asp-31 in the *Rhodobacter capsulatus* [5] and Leu-21 in the bovine [53] bc_1 complexes interact with His-202 of the same monomer just as Tyr-16 does in the yeast enzyme, and the role of yeast Tyr-9 in contacting the vicinity of the opposite center N is taken by Leu-21 in bacteria. Vertebrate bc_1 structures are too disordered in the region corresponding to Tyr-9 in yeast to identify the precise interaction with the other monomer [1–3], although the high degree of movement in this region could reflect a dynamic role of this amino-terminal helix in relaying conformational information between monomers [53].

4. Inter-monomeric electron equilibration between cytochrome *b* subunits

4.1 Theoretical calculations involving electron equilibration between center N sites via the b_L hemes

The possibility of electron transfer between the cytochrome *b* subunits in the dimer had been considered as a possible explanation for kinetic results even before the structure of the enzyme

was known [12,54], although it was assumed that equilibration could occur directly between the b_H hemes. The first crystal structure of the bc_1 complex that became available revealed that the distance between the b_L hemes, but not between the b_H hemes, was short enough to permit electron transfer between monomers [55]. As shown in Fig. 8 for the yeast dimer [4], the edge-to-edge distance between the b_L hemes is 13.8 Å, which is not too far from the 12.4 Å that separate the b_L and b_H hemes in each monomer. According to the simplified equation for the calculation of electron transfer rates when redox centers have the same potential [56], a distance of 13.8 Å would allow a tunneling rate of $3.27 \times 10^4\ s^{-1}$. This is more than 100 times faster than the maximum rate of quinol oxidation measured in the yeast bc_1 complex, which is $\sim 3 \times 10^2\ s^{-1}$ [57]. Thus, on the basis of distance considerations, electron equilibration between monomers via the b_L hemes can be expected to occur continuously between catalytic events at center P. However, the higher redox potential of the b_H heme makes it more probable for an electron residing in a b_L heme to be transferred to center N of its own monomer. The calculated rate of b_L to b_H electron tunneling for yeast can be estimated to be $\sim 1.3 \times 10^6\ s^{-1}$ based on the equation for calculating an exergonic electron transfer [56]. Therefore, the question arises of whether electron equilibration between center N sites (or between center P in one monomer and center N in the other) is relevant in comparison to the bc_1 complex turnover rate.

We have presented simulations showing the timescale at which an electron residing in one b_H heme in the dimer would equilibrate into the opposite monomer using a range of rates for each individual electron transfer between hemes [45]. We showed that intra-dimer equilibration could occur within 40 ms even at the slowest rates assumed. Others have addressed this issue using rates calculated from electron tunneling equations [56,58] and concluded that inter-monomeric electron transfer is expected to be relevant especially under physiological conditions in which an electrochemical potential across the membrane decreases the tendency of electrons to move from b_L to b_H, or when the b_H heme is pre-reduced by reverse electron transfer at center N.

The simulation shown in Fig. 9 uses the simple equilibration model between the four *b* hemes in the dimer that we have described previously [45], but with electron tunneling rates calculated from the distance and redox potential parameters of the yeast enzyme. Assuming E_m values of 80 mV for b_H and −50 mV for b_L (ΔE_m = 130 mV [56]), Fig. 9 shows that, even in the absence of a trans-membrane potential, an electron originally residing in one b_H heme should equilibrate to the other monomer within 10 ms (solid lines). This estimate results from using an equation for calculating the rate of the endergonic b_H to b_L electron transfer that is different from the exergonic b_L to b_H step [59]. If the exergonic equation is used to calculate both tunneling events, as has recently been proposed [60], the b_H to b_L transfer changes from $8.9 \times 10^3\ s^{-1}$ to $3.2 \times 10^4\ s^{-1}$. The net result of this different approach is a faster b_H to b_H equilibration that is complete within 3 ms (dotted lines in Fig. 9), roughly equivalent to the time-scale of maximal quinol oxidation at center P in the yeast enzyme ($\sim 300\ s^{-1}$). It is noteworthy that the K_{eq} for the one-electron sharing between b_H and b_L resulting from the two calculations is quite different (40.6 compared to 146.1 using the lower and higher b_H to b_L transfer rates, respectively). Still, equilibration between the four *b* hemes in the dimer would be completed within 10 ms in both scenarios.

Using data obtained with the bacterial bc_1 complex in chromatophores [61], it has been shown that the K_{eq} for electron transfer between the two *b* hemes in a monomer is much lower (10–25) than would be predicted from the Boltzmann distribution of one electron between two redox centers separated by 130–140 mV (K_{eq} ~200), implying Coulombic interactions between the hemes. This seems to be supported experimentally by the increase of 70–80 mV in the redox potential of the b_L heme when either one of the histidines that coordinates the b_H heme is mutated, resulting in the absence of b_H in the enzyme [62]. However, it should be pointed out that, on purely theoretical grounds, it is impossible for the equilibration of one electron

between the b_H and b_L hemes to be influenced by any electrostatic (Coulombic) effect of the ferro-b_H heme on the ferri-b_L heme. This is because movement of the electron from the reduced b_H heme to the oxidized b_L heme would eliminate the putative source of the Coulombic effect in the b_H heme as it becomes oxidized. Therefore, the fact that the redox potential of the b_L heme is in reality only 50–60 mV lower than that of the b_H heme implies a K_{eq} ~10 for the distribution of a single electron between the *b* hemes in a monomer. Obviously, this value would allow even faster equilibration between the two b_H hemes in the dimer than what is shown in Fig. 9, since the electron would reside a longer period of time in the b_L hemes. Nevertheless, the simulations we show in Fig. 9 using tunneling rate calculations indicate that, even at significantly higher K_{eq} values of >100 resulting from a slower b_H to b_L electron transfer, fast electron equilibration via the b_L hemes in the dimer would still be expected.

4.2 Experimental evidence for fast inter-monomeric electron transfer

The crystal structure of the bc_1 complex shows that the space between the b_L hemes is occupied by three aromatic residues, one of which (Phe-195 in *Rhodobacter sphaeroides*) has been proposed to be relevant for electron equilibration between monomers [63]. Mutation of this residue to alanine increased the rate of superoxide generation by the bc_1 complex three-fold, while decreasing the catalytic activity by ~20%. However, it was not directly shown that this mutation affected electron equilibration between cytochrome *b* subunits. Moreover, electron tunneling is generally considered to be dependent on distance and driving force, more than on the particular residues located in the space separating redox groups [59]. Therefore, it is possible that the Phe-195 mutation in the bacterial enzyme induces a change in the overall conformation of center P, or even modifies the redox potential of the b_L hemes, resulting in increased electron leakage to oxygen when quinol is oxidized.

We have obtained more direct evidence for intra-dimer electron transfer by using the experimental approach shown in Fig. 10 [45]. When antimycin is added in substoichiometric concentrations, a fraction of the bc_1 complex dimers will bind the inhibitor at only one center N. If quinol is then added to this population of dimers (previously blocked at center P by adding a stoichiometric concentration of myxothiazol), the b_H heme will undergo reduction through the uninhibited center N and semiquinone will be formed. As shown in Fig. 10A, the b_H heme at the center N where antimycin is bound will not undergo reduction unless it is able to equilibrate with the uninhibited center N in the other monomer via b_L to b_L electron transfer. If the electron reaches the inhibited center N, antimycin will modify the spectrum of its ferro-b_H heme, and a corresponding red shift will be detected.

As shown in Fig. 10B, where data from Ref. 45 is reproduced, this is exactly what we observed, with the relative amplitude of the red shift induced by antimycin corresponding to the calculated proportion of dimers with only one antimycin bound at center N. This experiment reports electron transfer between monomers if antimycin, a tightly bound inhibitor, is assumed not to dissociate from the oxidized center N and rebind to the quinol-reduced site in the other monomer during the timescale of the assay, which was <1 s. We excluded this possibility by showing that fast dissociation rates for antimycin would preclude the observed inhibition of b_H reduction at center N at stoichiometric concentrations [45]. We also measured the association rate constant for antimycin binding, and from this value and the K_d we calculated a very slow dissociation rate of ~10^{-5} s^{-1} [45].

Even considering that the effective concentration of antimycin in the detergent micelles is higher than that calculated for the total aqueous solution volume, this would mainly affect the value of those parameters expressed in units of concentration, such as the K_d and the association rate constant. The effective dissociation rate, which is expressed only in units of time, would still be very low. A low off rate has been experimentally demonstrated for funiculosin in the bovine bc_1 complex [64] and for ilicicolin in the yeast enzyme [65]. When these inhibitors are

bound to center N, they dissociate on a time scale of tens of minutes as measured by the change in spectral shift of the b_H heme upon addition of antimycin. Funiculosin and ilicicolin have K_d values 1–3 orders of magnitude higher than antimycin, implying that the dissociation rate constant for antimycin is even lower, at least as low as our estimated value of 10^{-5} s^{-1}. The argument that antimycin might dissociate from center N into the lipid or detergent phase much faster than into the aqueous volume in which K_d determinations are made [54] is also disproved by the extremely slow exchange between funiculosin or ilicicolin and antimycin when these are mixed together in the bc_1 phospholipid/detergent micelle [64,65], since these are all highly hydrophobic inhibitors.

For antimycin to bind to the quinol-reduced center N site and induce a spectral shift in the absence of inter-monomeric electron transfer, semiquinone would need to vacate the site where it was formed on a millisecond time scale. This contradicts the strong stabilization of semiquinone at center N, which behaves as a tightly bound ligand. Therefore, the result shown in Fig. 10 is direct evidence for fast electron equilibration between the center N sites in the dimer by means of b_L to b_L electron tunneling. Additional evidence was obtained from the non-linear inhibition of the extent of cytochrome *b* reduction by antimycin [45], and as mentioned previously (see Fig. 5 and Fig. 6), from the kinetic modeling of the partial inhibition by quinone [41].

The kinetics traces and simulations that are shown in Fig. 11 and taken from Ref. 15 make it evident that cytochrome *b* reduction through quinol oxidation at center P can be explained only if electrons are able to rapidly equilibrate between the cytochrome *b* subunits in the dimer. We have shown that, when center N sites are fully blocked with antimycin, the extent of cytochrome *b* reduced by quinol can be accurately simulated by assuming that two turnovers at one center P reduce both b_H hemes in the dimer, concomitantly with the reduction of cytochrome c_1 and the Rieske protein in the active monomer, after which no more turnovers can occur due to the lack of acceptors in the high potential chain of the active center P (Fig. 11A and Ref. 15). In contrast, the assumption that electrons remain only in the active monomer results in a lower amount of cytochrome *b* reduction than is observed, even if b_L is allowed to undergo reduction (pink dashed traces in Fig. 11B). In agreement with the modeling of cytochrome c_1 reduction kinetics explained before (see Fig. 2), significantly more cytochrome *b* reduction than observed should be expected if both center P sites are assumed to be active (blue solid traces in Fig. 11B). Overall, these results confirm the functional relevance of the close b_L to b_L distance observed in the bc_1 structures.

The linear decrease in the extent of b_H reduction at substoichiometric concentrations of myxothiazol that has apparently been found in the bacterial bc_1 complex in the presence of saturating antimycin has been used as an argument against electron transfer between monomers [66]. The rationale of this argument, which predicts a hyperbolic titration curve if there is electron transfer between monomers, is incorrect. Assuming that only one of the center P sites in the dimer is active in the presence of antimycin [15,18,28] and that myxothiazol is able to bind with the same affinity to both the active and the inactive monomers as shown by our data [18,28], linear titrations would also be obtained even if there exists intra-dimeric electron transfer. This is because an uninhibited dimer with only one active center P site would generate the same extent of b_H reduction as that produced by 50% of the dimers with one myxothiazol bound (those with the inhibitor in the already inactive monomer). The other 50% of the dimers, those having myxothiazol at the single active site, would generate no b_H reduction, the same as in the dimers with two myxothiazol molecules bound. When averaged over the enzyme population, the net result of these two binding scenarios would be a directly proportional loss of b_H reduction as a function of inhibitor concentration that would result in a linear titration curve reaching a value of zero at a ratio of one myxothiazol per monomer. The observation that myxothiazol does generate a non-linear inhibition of the extent of cytochrome *b* (and c_1)

reduction in the bc_1 complex from *Neurospora crassa* [54], suggests that in some species the inactive monomer can be switched on when the active one is inhibited, making the effect of electron equilibration between monomers more evident.

5. Physiological significance of the regulatory interactions within the bc_1 complex dimer

Regulation of the quinol and quinone binding sites along with inter-monomer electron transfer in the bc_1 dimer confers the advantage of allowing maximal quinol oxidation at center P in spite of the unavoidable reverse reactions that occur as semiquinone is stabilized at center N [41]. We have shown by simulations [45] that if the bc_1 complex functioned as an independent monomer, direct b_H reduction concomitant to the formation of a tightly bound semiquinone at center N would be favored at higher quinol/quinone ratios, resulting in an increased potential for center P inhibition and electron leakage to oxygen.

This situation can be experimentally mimicked by titrating the steady-state activity of the bc_1 complex with substoichiometric concentrations of antimycin, as shown in the data of Fig. 12, taken from Ref. 15. As antimycin concentration increases, a fraction of center N sites equal to the concentration of the inhibitor is blocked, preventing electrons to leave cytochrome *b*. If each monomer functioned independently, center P catalysis would come to a stop after at most two turnovers once the inhibitor blocked the center N site in that particular monomer. This would result in a linear decrease of the steady-state activity of the enzyme as a function of antimycin concentrations (green line in Fig. 12). The experimental points (solid circles) clearly do not follow this behavior, showing instead an increase in the catalytic activity when ~25% of the center N sites are blocked with antimycin. It should be noted that this apparent activation cannot be explained by alternative models that assume that the non-linear titration curves with antimycin are due to a fast movement of the inhibitor directly between center N sites [54], for which there is no structural support, since the crystal structures do not show any channel that would allow direct interchange of center N ligands between monomers [1–5,13].

Inter-monomer electron transfer by itself would allow the two center P sites in the dimer to recycle electrons out of cytochrome *b* through a single center N site, resulting in an increased resistance of the activity to antimycin (blue curve in Fig. 12A). However, the experimental data can only be explained by a model in which only half of the center P sites function in the absence of antimycin and if simultaneous catalysis at both center P sites occurs upon binding of one inhibitor per dimer (red curve in Fig. 12A). This comes from the assumption that those dimers occupied by one antimycin (red curve in Fig. 12B) contribute twice as much to the total activity as do the uninhibited dimers (blue curve in Fig. 12B). Electron transfer between the two monomers is also a condition in this mechanism, allowing electrons from the two active center P sites to leave cytochrome *b* through the uninhibited center N site. The result of this dimeric mode of bc_1 complex catalysis is that the net activity of quinol oxidation is fully resistant to a blockage of up to 50% of the center N sites, highlighting the physiological relevance of this dimeric mechanism in minimizing inhibition of center P by backward reactions at center N.

Considering all of the experimental observations explained in this review, a model for the regulation of quinol oxidation in the dimeric bc_1 complex can be proposed as shown in Fig. 13 and previously discussed in Ref. 36. The first key feature in this mechanism is an inverse symmetry relation between center P and center N that allows only one Rieske protein to approach center P when both center N sites are either vacant (intermediate I in Fig. 13), or occupied by semiquinone (intermediate III). Conversely, both Rieske proteins would have access to quinol at center P when there is an asymmetry at center N in which semiquinone is bound to only one monomer (intermediates II and IV).

The second key feature of this dimeric mechanism is the rapid equilibration of electrons between the two cytochrome *b* subunits, which allows semiquinone stabilization at either (intermediates II and IV) or both center N sites (intermediate III), regardless of which center P the electrons come from. This intra-dimer electron transfer would favor the situation in which the dimer has both b_H hemes oxidized and adjacent to semiquinone (similar to intermediate III), which allows only one center P to be active. This state of the enzyme is optimal to avoid electron leakage to oxygen, since it presents six potential acceptors (two b_L hemes, two b_H hemes and two semiquinones) for electrons coming from quinol oxidation at center P.

The state in which both center P sites are able to oxidize quinol simultaneously (intermediates II and IV) might create the risk of too many electrons being delivered into cytochrome *b*. However, b_H reduction at the vacant center N by reverse quinol oxidation (not shown in Fig. 13) would be prevented by rendering stabilization of a second semiquinone unfavorable as long as both Rieske proteins are in a catalytically competent configuration (see Fig. 6). Furthermore, the high mobility of the Rieske protein domain [37] would make it unlikely for a conformation with two Rieske proteins in the vicinity of center P to be a stable intermediate. Even if the configuration in which simultaneous catalysis at center P occurs is stabilized by binding one antimycin per dimer (see Fig. 12), electron transfer between monomers and the fast rate of reactions at center N would allow electrons to leave through one cytochrome *b* monomer. Nevertheless, in the absence of inhibitors, center N reactions would favor a fast transition towards the conformation that has only one active center P (intermediates I and III).

The brief intervals during which only one semiquinone is occupying center N in a dimer (intermediates II and IV) would allow the previously inactive center P to reach a catalytically active conformation with the Rieske protein approaching the substrate (intermediates II and IV). Which of the two center P sites oxidizes quinol first would be a matter of random chance, resulting in the two center P sites undergoing the same number of turnovers on average. Thus, this is an alternating sites mechanism of quinol oxidation [67], although each monomer would not necessarily become inactive after a fixed number of turnovers to allow activity in the second site. This is emphasized in Fig. 13 by the black and gray arrows, which represent equally probable electron pathways and ligand binding or dissociation events that would result in conversions between dimer conformations. Whether a particular dimer intermediate follows a conversion pathway indicated by a black or by a gray arrow would depend on the particular redox state of each b_H heme at the time of a quinol oxidation event, which would favor the electron ending up in the same monomer or in the opposite one by b_L to b_L mediated transfer.

This proposed mechanism of stochastically-alternating center P sites controlled by semiquinone stabilization at center N would confer significant flexibility to the bc_1 complex dimer. Its main advantage would be to allow quinol oxidation to proceed unhindered by reverse center N reactions, resulting in enhanced resilience to different quinol/quinone ratios and trans-membrane potentials generated by the variable energetic conditions of the respiratory chain. Only in the presence of very high (and possibly non-physiological) electrochemical gradients would center P slow down and start to leak electrons to oxygen due to the tendency of electrons to stay in the b_L hemes. The highly damaging reactions that would ensue if the bc_1 complex did not have regulatory mechanisms to minimize oxygen radical formation constitute a strong selective pressure that explains the strict conservation of the dimeric structure of this enzyme throughout the evolution of aerobic organisms.

References

1. Zhang ZL, Huang LS, Shulmeister VM, Chi YI, Kim KK, Hung LW, Crofts AR, Berry EA, Kim SH. Electron transfer by domain movement in cytochrome bc_1. Nature 1998;392:677–684. [PubMed: 9565029]

2. Yu CA, Xia D, Kim H, Deisenhofer J, Zhang L, Kachurin AM, Yu L. Structural basis of functions of the mitochondrial bc_1 complex. Biochim. Biophys. Acta 1998;1365:151–158. [PubMed: 9693733]
3. Iwata S, Lee JW, Okada K, Lee JK, Iwata M, Rasmussen B, Link TA, Ramaswamy S, Jap BK. Complete structure of the 11-subunit bovine mitochondrial cytochrome bc_1 complex. Science 1998;281:64–71. [PubMed: 9651245]
4. Hunte C, Koepke J, Lange C, Rossmanith T, Michel H. Structure at 2.3 Å resolution of the cytochrome bc_1 complex from the yeast *Saccharomyces cerevisiae* co-crystallized with an antibody Fv fragment. Structure 2000;8:669–684. [PubMed: 10873857]
5. Berry EA, Huang LS, Saechao LK, Pon NG, Valkova-Valchanova M, Daldal F. X-Ray Structure of *Rhodobacter capsulatus* cytochrome bc_1: Comparison with its mitochondrial and chloroplast counterparts. Photosynth. Res 2004;81:251–275. [PubMed: 16034531]
6. Mitchell P. Possible molecular mechanisms of the protonmotive function of cytochrome systems. J. Theor. Biol 1976;62:327–367. [PubMed: 186667]
7. Brandt U, Trumpower B. The protonmotive Q cycle in mitochondria and bacteria. Crit. Rev. Biochem. Mol. Biol 1994;29:165–197. [PubMed: 8070276]
8. Ohnishi T, Trumpower BL. Differential effects of antimycin on ubisemiquinone bound in different environments in isolated succinate-cytochrome c reductase complex. J. Biol. Chem 1980;255:3278–3274. [PubMed: 6245075]
9. De Vries S, Berden JA, Slater EC. Properties of a semiquinone anion located in the QH_2:cytochrome c oxidoreductase segment of the mitochondrial respiratory chain. FEBS Lett 1980;122:143–148. [PubMed: 7215541]
10. Robertson DE, Prince RC, Bowyer JR, Matsuura K, Dutton PL, Ohnishi T. Thermodynamic properties of the semiquinone and its binding site in the ubiquinol-cytochrome c (c_2) oxidoreductase of respiratory and photosynthetic systems. J. Biol. Chem 1984;259:1758–1763. [PubMed: 6319410]
11. Kramer DM, Roberts AG, Muller F, Cape J, Bowman MK. Q-cycle bypass reactions at the Qo site of the cytochrome bc_1 (and related) complexes. Methods Enzymol 2004;382:21–45. [PubMed: 15047094]
12. De Vries S, Albracht SP, Berden JA, Slater EC. The pathway of electrons through QH_2:cytochrome c oxidoreductase studied by pre-steady-state kinetics. Biochim. Biophys. Acta 1982;681:41–53. [PubMed: 6288082]
13. Gao X, Wen X, Esser L, Quinn B, Yu L, Yu CA, Xia D. Structural basis for the quinone reduction in the bc_1 complex: a comparative analysis of crystal structures of mitochondrial cytochrome bc_1 with bound substrate and inhibitors at the Qi site. Biochemistry 2003;42:9067–9080. [PubMed: 12885240]
14. Crofts AR, Shinkarev VP, Kolling DR, Hong S. The modified Q-cycle explains the apparent mismatch between the kinetics of reduction of cytochromes c_1 and b_H in the bc_1 complex. J. Biol. Chem 2003;278:36191–36201. [PubMed: 12829696]
15. Covian R, Gutierrez-Cirlos EB, Trumpower BL. Anti-cooperative oxidation of ubiquinol by the yeast cytochrome bc_1 complex. J. Biol. Chem 2004;279:15040–15049. [PubMed: 14761953]
16. Meinhardt SW, Crofts AR. The role of cytochrome b_{566} in the electron transfer of *Rhodopseudomonas sphaeroides*. Biochim. Biophys. Acta 1983;723:219–230.
17. Wikstrom MK, Berden JA. Oxidoreduction of cytochrome b in the presence of antimycin. Biochim. Biophys. Acta 1972;283:403–420. [PubMed: 4346389]
18. Covian R, Kleinschroth T, Ludwig B, Trumpower BL. Asymmetric binding of stigmatellin to the dimeric *Paracoccus denitrificans* bc_1 complex. Evidence for anti-cooperative ubiquinol oxidation and communication between center P ubiquinol oxidation sites. J. Biol. Chem 2007;282:22289–22297. [PubMed: 17561507]
19. Gennis RB, Barquera B, Hacker B, Van Doren SR, Arnaud S, Crofts AR, Davidson E, Gray KA, Daldal F. The bc1 complexes of *Rhodobacter sphaeroides* and *Rhodobacter capsulatus*. J. Bioenerg. Biomembr 1993;25:195–209. [PubMed: 8394316]
20. Mulkidjanian AY. Proton translocation by the cytochrome bc_1 complexes of prototrophic bacteria: introducing the activated Q-cycle. Photochem. Photobiol. Sci 2007;6:19–34. [PubMed: 17200733]

21. Gopta OA, Feniouk BA, Junge W, Mulkidjanian AY. The cytochrome *bc*1 complex of Rhodobacter capsulatus: ubiquinol oxidation in a dimeric Q-cycle? FEBS Lett 1998;431:291–296. [PubMed: 9708922]
22. Snyder CH, Gutierrez-Cirlos EB, Trumpower BL. Evidence for a concerted mechanism of ubiquinol oxidation by the cytochrome bc_1 complex. J. Biol. Chem 2000;275:13535–13541. [PubMed: 10788468]
23. Guergova-Kuras M, Kuras R, Ugulava N, Hadad I, Crofts AR. Specific mutagenesis of the rieske iron-sulfur protein in *Rhodobacter sphaeroides* shows that both the thermodynamic gradient and the pK of the oxidized form determine the rate of quinol oxidation by the bc_1 complex. Biochemistry 2000;39:7436–7444. [PubMed: 10858292]
24. Forquer I, Covian R, Bowman MK, Trumpower BL, Kramer DM. Similar transition states mediate the Q-cycle and superoxide production by the cytochrome bc_1 complex. J. Biol. Chem 2006;281:38459–38465. [PubMed: 17008316]
25. Hong S, Ugulava N, Guergova-Kuras M, Crofts AR. The energy landscape for ubihydroquinone oxidation at the Qo site of the bc1 Complex in *Rhodobacter sphaeroides*. J. Biol. Chem 1999;274:33931–33944. [PubMed: 10567355]
26. Brandt U, Haase U, Schägger H, von Jagow G. Significance of the "Rieske" iron-sulfur protein for formation and function of the ubiquinol-oxidation pocket of mitochondrial cytochrome c reductase (bc_1 complex). J. Biol. Chem 1991;266:19958–19964. [PubMed: 1657909]
27. Esser L, Quinn B, Li YF, Zhang M, Elberry M, Yu L, Yu CA, Xia D. Crystallographic studies of quinol oxidation site inhibitors: a modified classification of inhibitors for the cytochrome bc_1 complex. J. Mol. Biol 2004;341:281–302. [PubMed: 15312779]
28. Gutierrez-Cirlos EB, Trumpower BL. Inhibitory analogs of ubiquinol act anti-cooperatively on the yeast cytochrome bc_1 complex. Evidence for an alternating, half-of-the-sites mechanism of ubiquinol oxidation. J. Biol. Chem 2002;277:1195–1202. [PubMed: 11700316]
29. Covian R, Pardo JP, Moreno-Sanchez R. Tight binding of inhibitors to bovine bc_1 complex is independent of the Rieske protein redox state. J. Biol. Chem 2002;277:48449–48455. [PubMed: 12364330]
30. Brandt U, von Jagow G. Analysis of inhibitor binding to the mitochondrial cytochrome c reductase by fluorescence quench titration. Evidence for a 'catalytic switch' at the Qo center. Eur. J. Biochem 1991;195:163–170. [PubMed: 1991466]
31. Darrouzet E, Valkova-Valchanova M, Daldal F. The [2Fe-2S] cluster E_m as an indicator of the iron-sulfur subunit position in the ubihydroquinone oxidation site of the cytochrome bc_1 complex. J. Biol. Chem 2002;277:3464–3470. [PubMed: 11707448]
32. Cooley JW, Roberts AG, Bowman MK, Kramer DM, Daldal F. The raised midpoint potential of the [2Fe2S] cluster of cytochrome bc_1 is mediated by both the Qo site occupants and the head domain position of the Fe-S protein subunit. Biochemistry 2004;43:2217–2227. [PubMed: 14979718]
33. Gutierrez-Cirlos EB, Merbitz-Zahradnik T, Trumpower BL. Failure to insert the iron-sulfur cluster into the Rieske iron-sulfur protein impairs both center N and center P of the cytochrome bc_1 complex. J. Biol. Chem 2002;277:50703–50709. [PubMed: 12377760]
34. Valkova-Valchanova M, Darrouzet E, Moomaw CR, Slaughter CA, Daldal F. Proteolytic cleavage of the Fe-S subunit hinge region of *Rhodobacter capsulatus* bc_1 complex: effects of inhibitors and mutations. Biochemistry 2000;39:15484–15492. [PubMed: 11112534]
35. Cooley JW, Ohnishi T, Daldal F. Binding dynamics at the quinone reduction (Qi) site influence the equilibrium interactions of the iron-sulfur protein and hydroquinone oxidation (Qo) site of the cytochrome bc_1 complex. Biochemistry 2005;44:10520–10532. [PubMed: 16060661]
36. Covian R, Trumpower BL. Regulatory interactions between ubiquinol oxidation and ubiquinone reduction sites in the dimeric cytochrome bc_1 complex. J. Biol. Chem 2006;281:30925–30932. [PubMed: 16908520]
37. Crofts AR, Hong S, Zhang Z, Berry EA. Physicochemical aspects of the movement of the Rieske iron-sulfur protein during quinol oxidation by the bc_1 complex from mitochondria and photosynthetic bacteria. Biochemistry 1999;38:15827–15839. [PubMed: 10625447]
38. Von Jagow G, Link TA. Use of specific inhibitors of the mitochondrial bc_1 complex. Methods Enzymol 1986;126:253–271. [PubMed: 2856132]

39. Rich PR, Jeal AE, Madgwick SA, Moody SJ. Inhibitor effects on redox-linked protonations of the *b* haems of the mitochondrial bc_1 complex. Biochim. Biophys. Acta 1990;1018:29–40. [PubMed: 2165418]
40. Kostyrko VA, Iaguzhinskii LS. Two sites of ubiquinone binding in mitochondrial succinate oxidase. Biokimiia 1979;44:1884–1890.
41. Covian R, Zwicker K, Rotsaert FA, Trumpower BL. Asymmetric and redox-specific binding of quinone and quinol at center N of the dimeric yeast cytochrome bc_1 complex. Consequences for semiquinone stabilization. J. Biol. Chem 2007;282:24198–24208. [PubMed: 17584742]
42. De Vries S, Albracht SP, Berden JA, Marres CA, Slater EC. The effect of pH, ubiquinone depletion and myxothiazol on the reduction kinetics of the prosthetic groups of ubiquinol:cytochrome *c* oxidoreductase. Biochim. Biophys. Acta 1983;723:91–103. [PubMed: 6299337]
43. Glaser EG, Meinhardt SW, Crofts AR. Reduction of cytochrome *b*-561 through the antimycin-sensitive site of the ubiquinol-cytochrome *c*2 oxidoreductase complex of *Rhodopseudomonas sphaeroides*. FEBS Lett 1984;178:336–342. [PubMed: 6096171]
44. Tsai AL, Kauten R, Palmer G. The interaction of yeast Complex III with some respiratory inhibitors. Biochim. Biophys. Acta 1985;806:418–426. [PubMed: 2982396]
45. Covian R, Trumpower BL. Rapid electron transfer between monomers when the cytochrome bc_1 complex dimer is reduced through center N. J. Biol. Chem 2005;280:22732–22740. [PubMed: 15833742]
46. De la Rosa FF, Palmer G. Reductive titration of CoQ-depleted Complex III from baker's yeast. Evidence for an exchange-coupled complex between QH. and low-spin ferricytochrome b. FEBS Lett 1983;163:140–143. [PubMed: 6313430]
47. Lange C, Hunte C. Crystal structure of the yeast cytochrome bc_1 complex with its bound substrate cytochrome c. Proc. Natl. Acad. Sci. U.S.A 2002;99:2800–2805. [PubMed: 11880631]
48. Esser L, Elberry M, Zhou F, Yu CA, Yu L, Xia D. Inhibitor-complexed structures from the photosynthetic bacterium *Rhodobacter sphaeroides*. J. Biol. Chem 2008;283:2846–2857. [PubMed: 18039651]
49. Wenz T, Covian R, Hellwig P, Macmillan F, Meunier B, Trumpower BL, Hunte C. Mutational analysis of cytochrome *b* at the ubiquinol oxidation site of yeast complex III. J. Biol. Chem 2007;282:3977–3988. [PubMed: 17145759]
50. Berry EA, Guergova-Kuras M, Huang L, Crofts AR. Structure and function of cytochrome *bc* complexes. Annu. Rev. Biochem 2000;69:1005–1075. [PubMed: 10966481]
51. Gray KA, Dutton PL, Daldal F. Requirement of histidine 217 for ubiquinone reductase activity (Qi site) in the cytochrome bc_1 complex. Biochemistry 1994;33:723–733. [PubMed: 8292600]
52. Kolling DR, Samoilova RI, Holland JT, Berry EA, Dikanov SA, Crofts AR. Exploration of ligands to the Qi site semiquinone in the bc_1 complex using high-resolution EPR. J. Biol. Chem 2003;278:39747–39754. [PubMed: 12874282]
53. Huang LS, Cobessi B, Tung EY, Berry EA. Binding of the respiratory chain inhibitor antimycin to the mitochondrial bc_1 complex: a new crystal structure reveals an altered intramolecular hydrogen-bonding pattern. J. Mol. Biol 2005;351:573–597. [PubMed: 16024040]
54. Bechmann G, Weiss H, Rich PR. Non-linear inhibition curves for tight-binding inhibitors of dimeric ubiquinol-cytochrome *c* oxidoreductases. Evidence for rapid inhibitor mobility. Eur. J. Biochem 1992;208:315–325. [PubMed: 1325904]
55. Xia D, Yu CA, Kim H, Xian JZ, Kachurin AM, Zhang L, Yu L, Deisenhofer J. Crystal structure of the cytochrome bc_1 complex from bovine heart mitochondria. Science 1997;277:60–66. [PubMed: 9204897]
56. Moser CC, Farid TA, Chobot SE, Dutton PL. Electron tunneling chains of mitochondria. Biochim. Biophys. Acta 2006;1757:1096–1109. [PubMed: 16780790]
57. Ljungdahl PO, Pennoyer JD, Trumpower BL. Purification of cytochrome bc_1 complexes from phylogenically diverse species by a single method. Methods Enzymol 1986;126:181–191. [PubMed: 2856125]
58. Shinkarev VP, Wraight CA. Intermonomer electron transfer in the bc_1 complex dimer is controlled by the energized state and by impaired electron transfer between low and high potential hemes. FEBS Lett 2007;581:1535–1541. [PubMed: 17399709]

59. Page CC, Moser CC, Chen XX, Dutton PL. Natural engineering principles of electron tunnelling in biological oxidation-reduction. Nature 1999;402:47–52. [PubMed: 10573417]

60. Crofts AR, Rose S. Marcus treatment of endergonic reactions: a commentary. Biochim. Biophys. Acta 2002;1767:1228–1232. [PubMed: 17720135]

61. Shinkarev VP, Crofts AR, Wraight CA. The electric field generated by photosynthetic reaction center induces rapid reversed electron transfer in the bc_1 complex. Biochemistry 2001;40:12584–12590. [PubMed: 11601982]

62. Yun CH, Crofts AR, Gennis RB. Assignment of the histidine axial ligands to the cytochrome b_H and cytochrome b_L components of the bc_1 complex from *Rhodobacter sphaeroides* by site-directed mutagenesis. Biochemistry 1991;30:6747–6754. [PubMed: 1648391]

63. Gong X, Yu L, Xia D, Yu CA. Evidence for electron equilibrium between the two hemes bL in the dimeric cytochrome bc_1 complex. J. Biol. Chem 2005;280:9251–9257. [PubMed: 15615714]

64. Kamensky Y, Konstantinov AA, Kunz WS, Surkov S. Effects of bc_1-site electron transfer inhibitors on the absorption spectra of mitochondrial cytochromes *b*. FEBS Lett 1985;181:95–99. [PubMed: 2982656]

65. Gutierrez-Cirlos EB, Merbitz-Zahradnik T, Trumpower BL. Inhibition of the yeast cytochrome bc_1 complex by ilicicolin H, a novel inhibitor that acts at the Qn site of the bc_1 complex. J. Biol. Chem 2004;279:8708–8714. [PubMed: 14670947]

66. Crofts AR, Berry EA. Structure and function of the cytochrome bc_1 complex of mitochondria and photosynthetic bacteria. Curr. Opin. Struct. Biol 1998;8:501–509. [PubMed: 9729743]

67. Trumpower BL. A concerted, alternating sites mechanism of ubiquinol oxidation by the dimeric cytochrome bc_1 complex. Biochim. Biophys. Acta 2002;1555:166–173. [PubMed: 12206910]

Fig. 1. Structure of the catalytic subunits of the yeast *bc*$_1$ complex dimer

Cytochrome *b* (green), the Rieske iron-sulfur protein (blue), and cytochrome c_1 (red) are colored in one monomer and shown as ribbons. Notice the tilted trans-membrane helix of the Rieske protein that is imbedded in one monomer and connects through a flexible linker region to the extrinsic iron-sulfur cluster containing domain that interacts with the other monomer. Redox centers (c_1, b_L and b_H hemes, and the FeS cluster), as well as the center P inhibitor stigmatellin (Stg) and the center N ubiquinone (Ubi) are shown as ball-and-stick models. The structure is taken from Protein Data Bank code 1EZV [4].

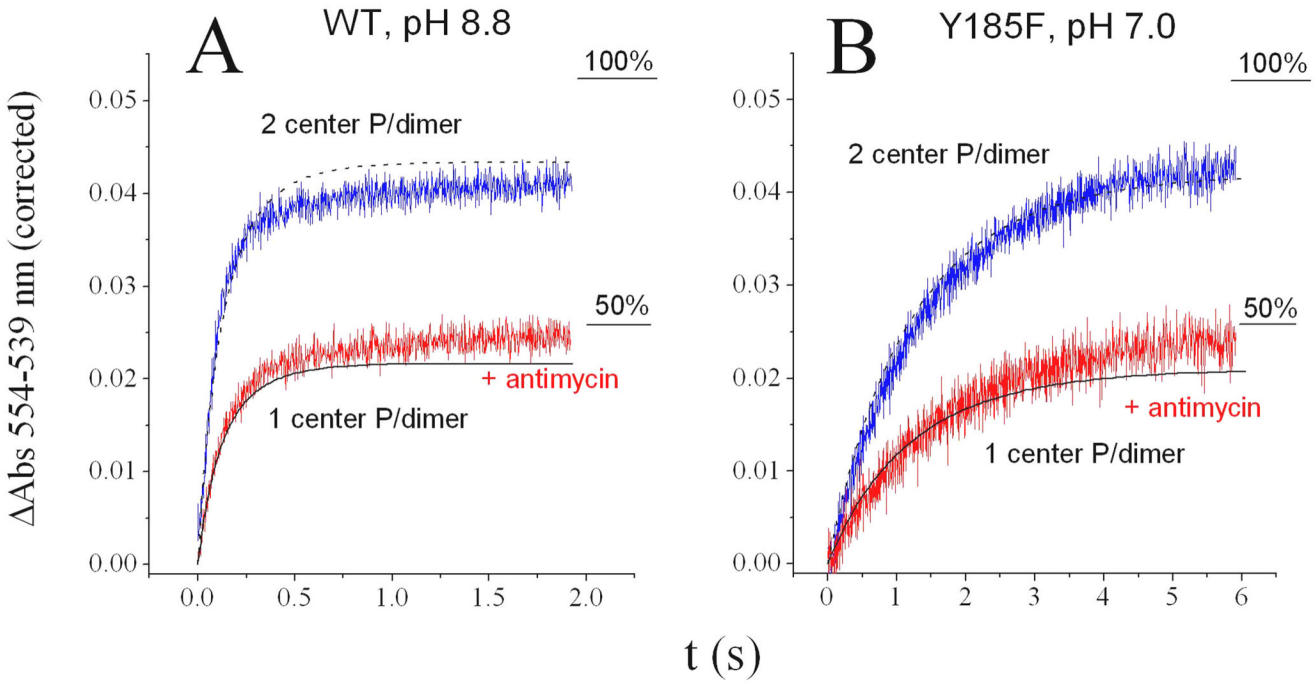

Fig. 2. Pre-steady state reduction of cytochrome c_1 in the yeast cytochrome bc_1 complex

Cytochrome bc_1 complex (3 μM) of wild-type yeast at pH 8.8 (A) or of the Y185F Rieske mutant at pH 7.0 (B) was rapidly mixed with 12 μM of decyl-ubiquinol in the presence (red traces) or absence (blue traces) of 6 μM antimycin. Contribution of cytochrome *b* absorbance at the indicated wavelengths was corrected for as described in Ref. 15. Black curves represent the simulated cytochrome c_1 reduction assuming that only one (solid line) or both (dotted line) center P sites catalyzed only one quinol oxidation reaction. Simulations also assumed ~80% occupancy of the electron in c_1 and ~20% in the Rieske protein. Data and simulations are reproduced from Ref. 15, where the full details of the kinetic modeling are provided.

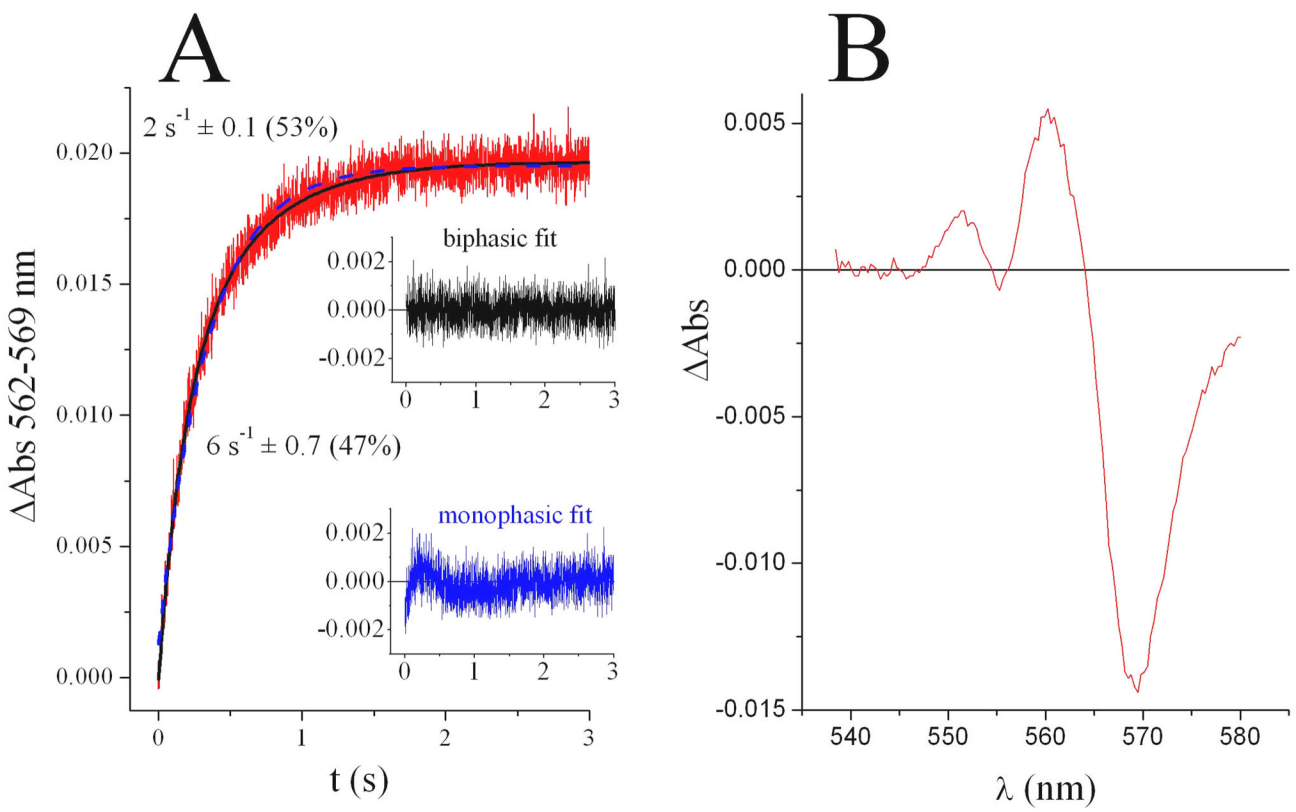

Fig. 3. Asymmetric binding of stigmatellin to the *Paracoccus denitrificans* cytochrome bc_1 complex

The time-dependent course of 15 μM stigmatellin binding to 2 μM reduced bc_1 complex (red trace in panel A) is fitted better (solid black curve) using a biphasic exponential function as compared to a monophasic equation (dotted blue curve), as shown by the corresponding residual plots in the insert. The rate of each binding phase obtained from the biphasic fit is shown in parentheses along with its relative contribution to the total spectral change. The change in the absorbance spectrum of the b_L heme generated by the binding of stigmatellin (panel B) is asymmetric, with a trough amplitude that is twice the magnitude of the peak. As described previously in Ref. 18, where data is taken from, most of the asymmetry is generated during the slow binding phase.

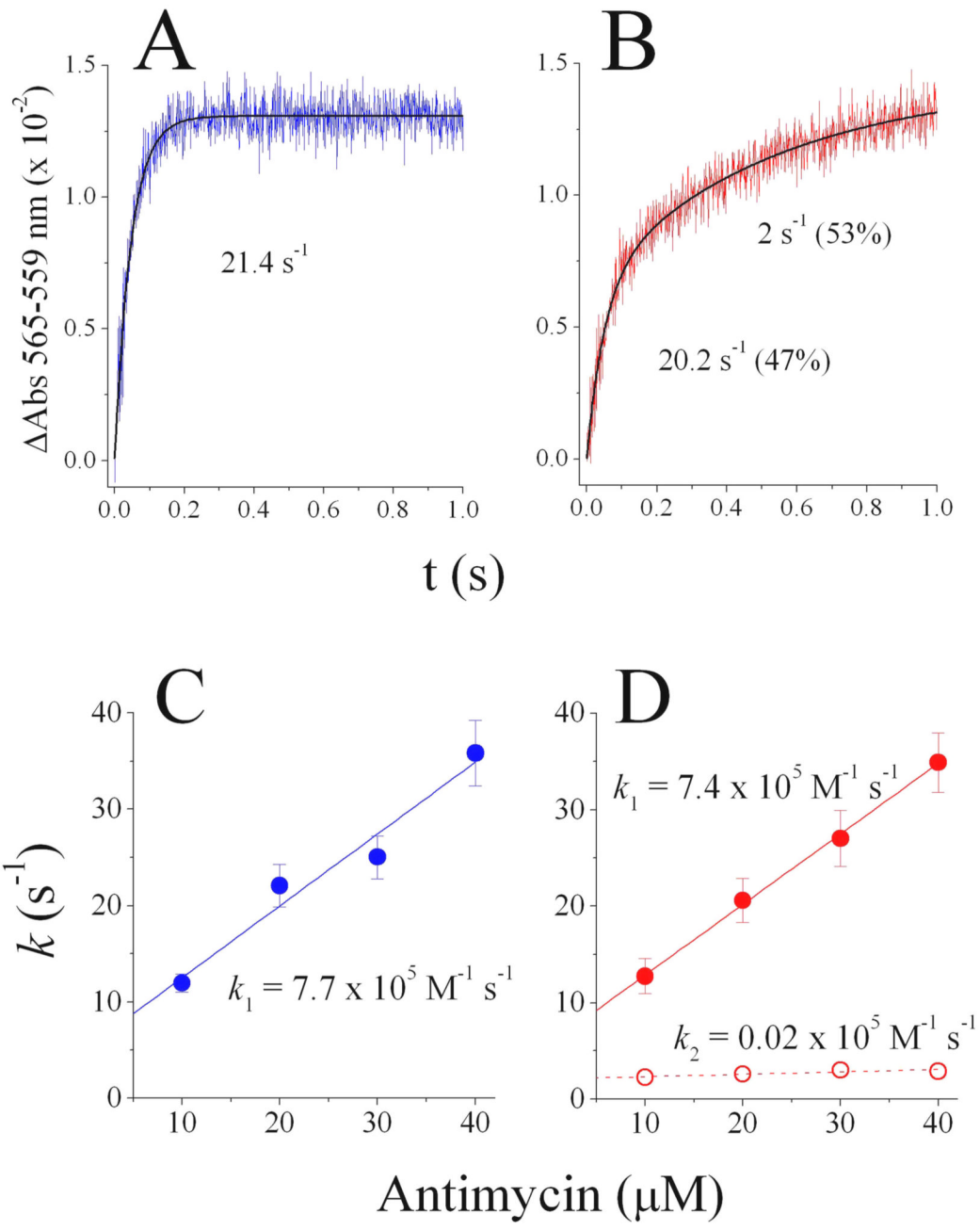

Fig. 4. Kinetics of antimycin binding to center N in the presence of center P inhibitors

Antimycin (20 μM) binds in a single phase in the presence of 1.2 equivalents of myxothiazol per bc_1 monomer, present at a concentration of 2.5 μM (panel A) and in two phases in the presence of stigmatellin (panel B). The relative contribution of each kinetic phase in panel B is shown in parentheses next to its rate. The single rate observed with myxothiazol bound at center P is linearly dependent on the concentration of antimycin (panel C). With stigmatellin occupying the center P sites (panel D) binding of antimycin is concentration-dependent during the first kinetic phase (filled red circles and solid red line), but is concentration-independent during the slow second phase (open red circles, dotted red line), indicating that a conformational

change limits binding of antimycin to half of the center N sites when stigmatellin is occupying both center P sites in the dimer. Data reproduced from Ref. 36.

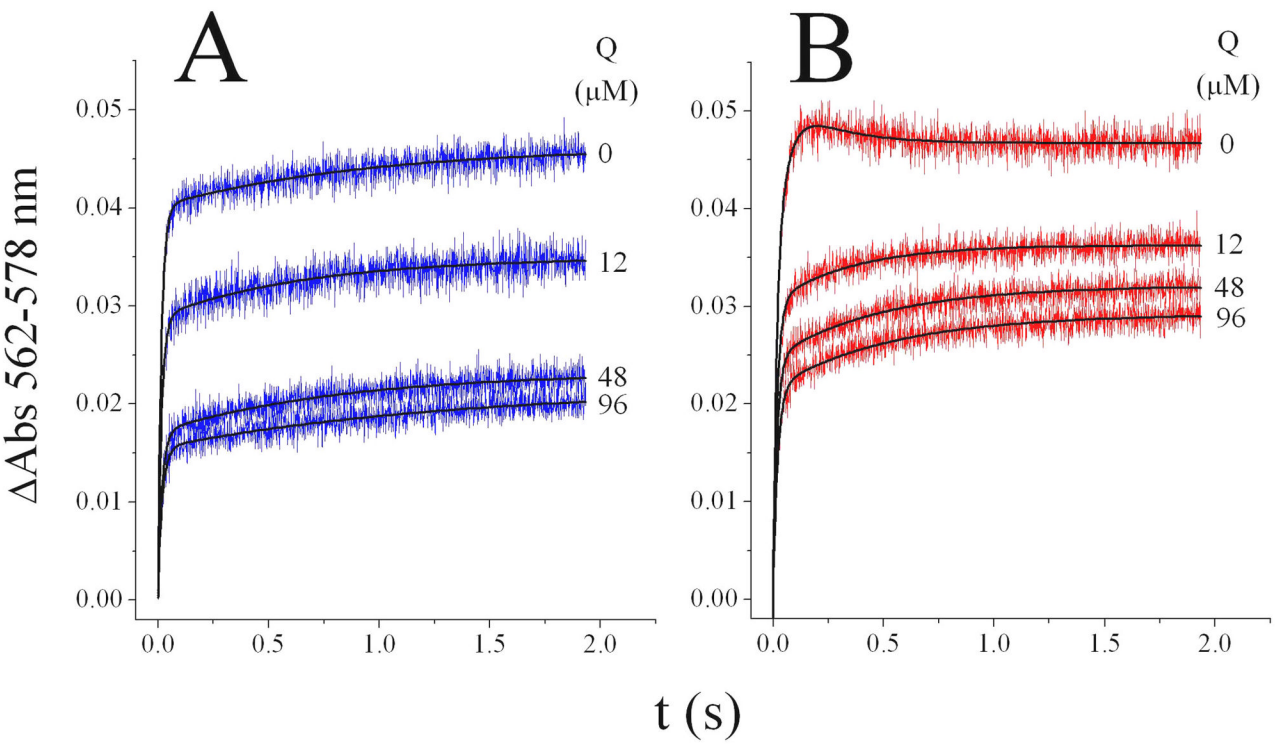

Fig. 5. Reduction of heme b_H through center N in the presence of center P inhibitors

Reduction of 1.5 μM yeast bc_1 complex by decyl-ubquinol (24 μM) was determined in the presence of 1.2 equivalents of myxothiazol (panel A) or stigmatellin (panel B) at different decyl-ubiquinone (Q) concentrations. The solid black lines represent the fit of each kinetic trace to a biphasic or triphasic function. Data reproduced from Ref. 41.

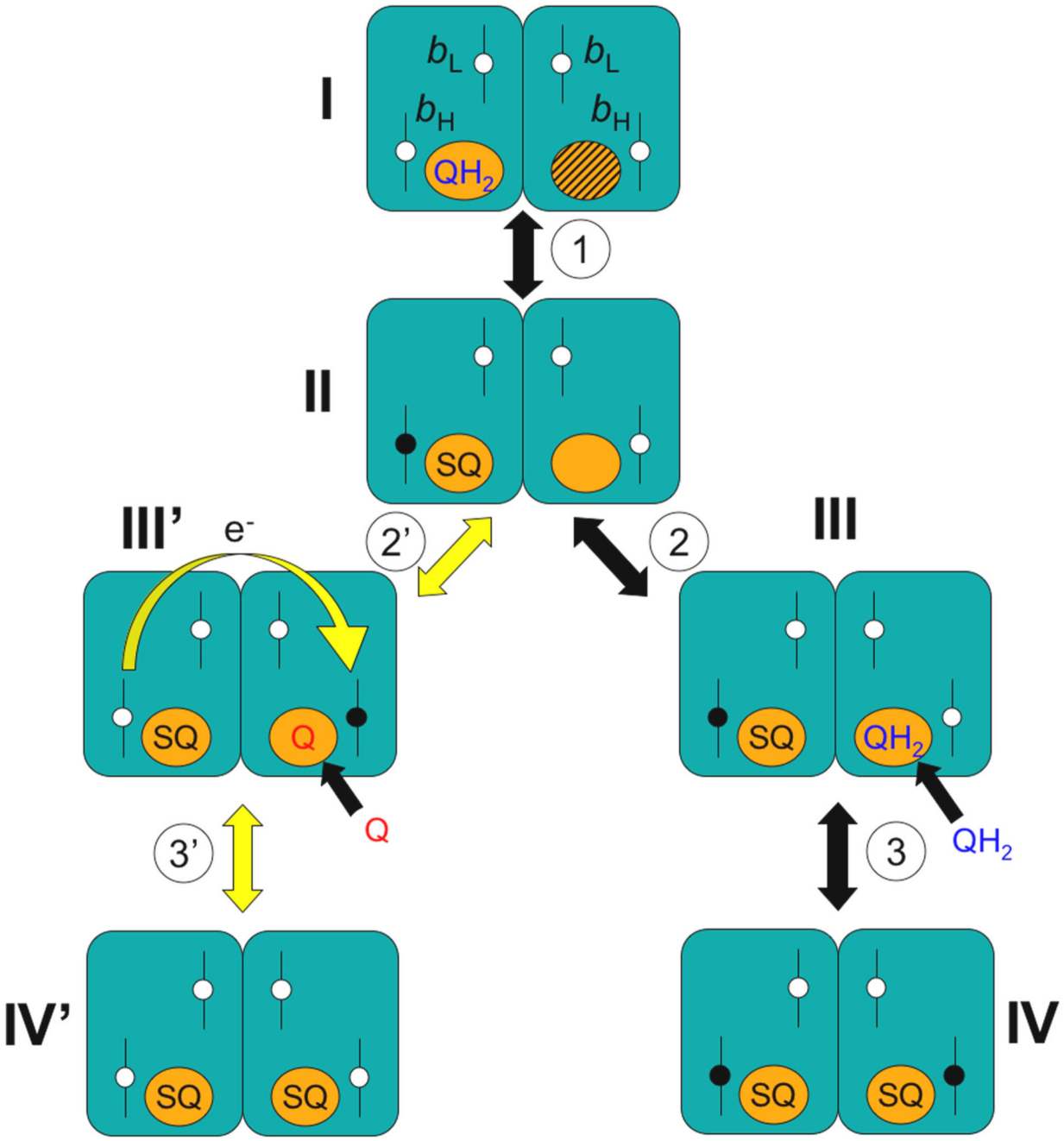

Fig. 6. Model of electron equilibration at center N in the dimeric bc_1 complex

Cytochrome *b* dimers are shown as paired rectangles with center N sites as circles next to the b_H hemes. All other subunits, as well as center P reactions, have been omitted for clarity. The model assumes that quinol (QH_2) binds only to center N sites with an oxidized (white) b_H heme, and that quinone (Q) binds exclusively when b_H is reduced (black). Semiquinone (SQ) formation is initially prevented in one center N (hatched circle in intermediate I). Solid arrows indicate changes that result from binding of a quinone or quinol ligand to a center N site or by electron transfer between heme and a ligand in one monomer. Yellow arrows, including the curved yellow arrow in intermediate III', indicate changes that depend on electron transfer from one b_H to the other via the b_L hemes as discussed more fully in the text.

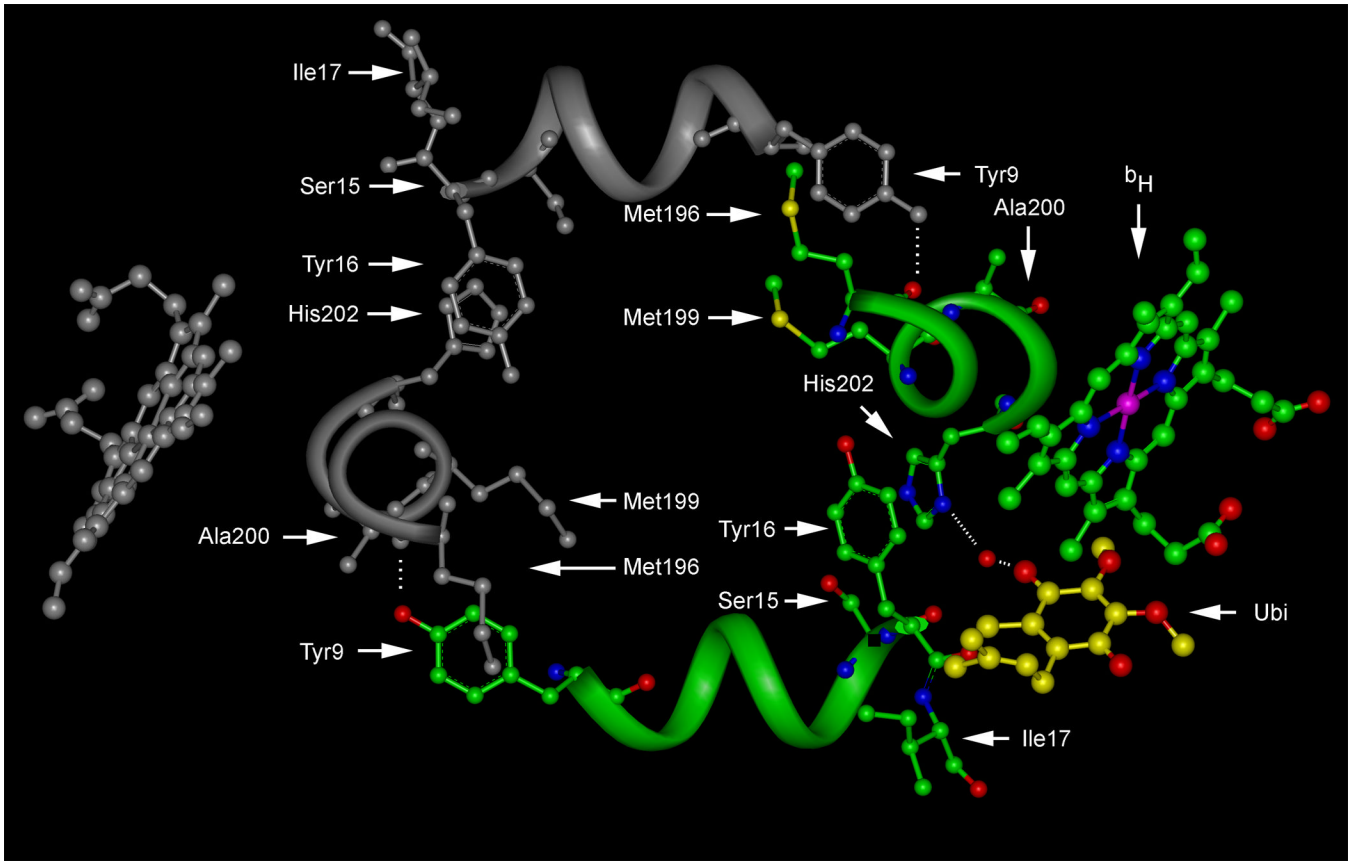

Fig. 7. Close-up view of a potential conformational communication pathway between center N sites in the yeast bc_1 complex dimer

Atoms and the backbone portions of helices are colored in only one monomer. Residues proposed to be important for inter-monomeric communication are indicated, along with the b_H heme and ubiquinone (Ubi) bound via a water mediated hydrogen bond to His-202 in the colored monomer. The structure is excerpted from the stigmatellin-bound bc_1 complex (Protein Data Bank code 1EZV [4]).

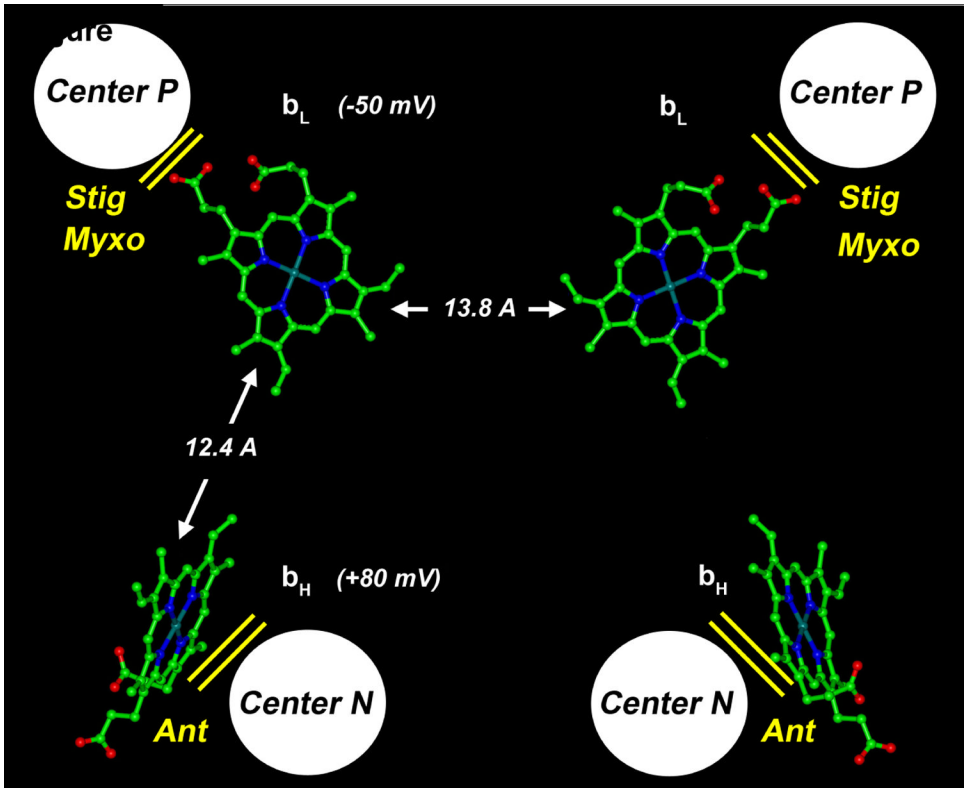

Fig. 8. Distances between hemes in the yeast bc_1 complex dimer

Edge-to-edge distances between heme tetra-pyrrole rings are indicated by arrows along with the heme redox midpoint potentials as measured in the isolated yeast bc_1 complex. The approximate locations of the center P and center N reaction sites are also shown with the respective inhibitors that block each site: stigmatellin (Stig), myxothiazol (Myxo), and antimycin (Anti). The structure was excerpted from PDB code 1EZV [4].

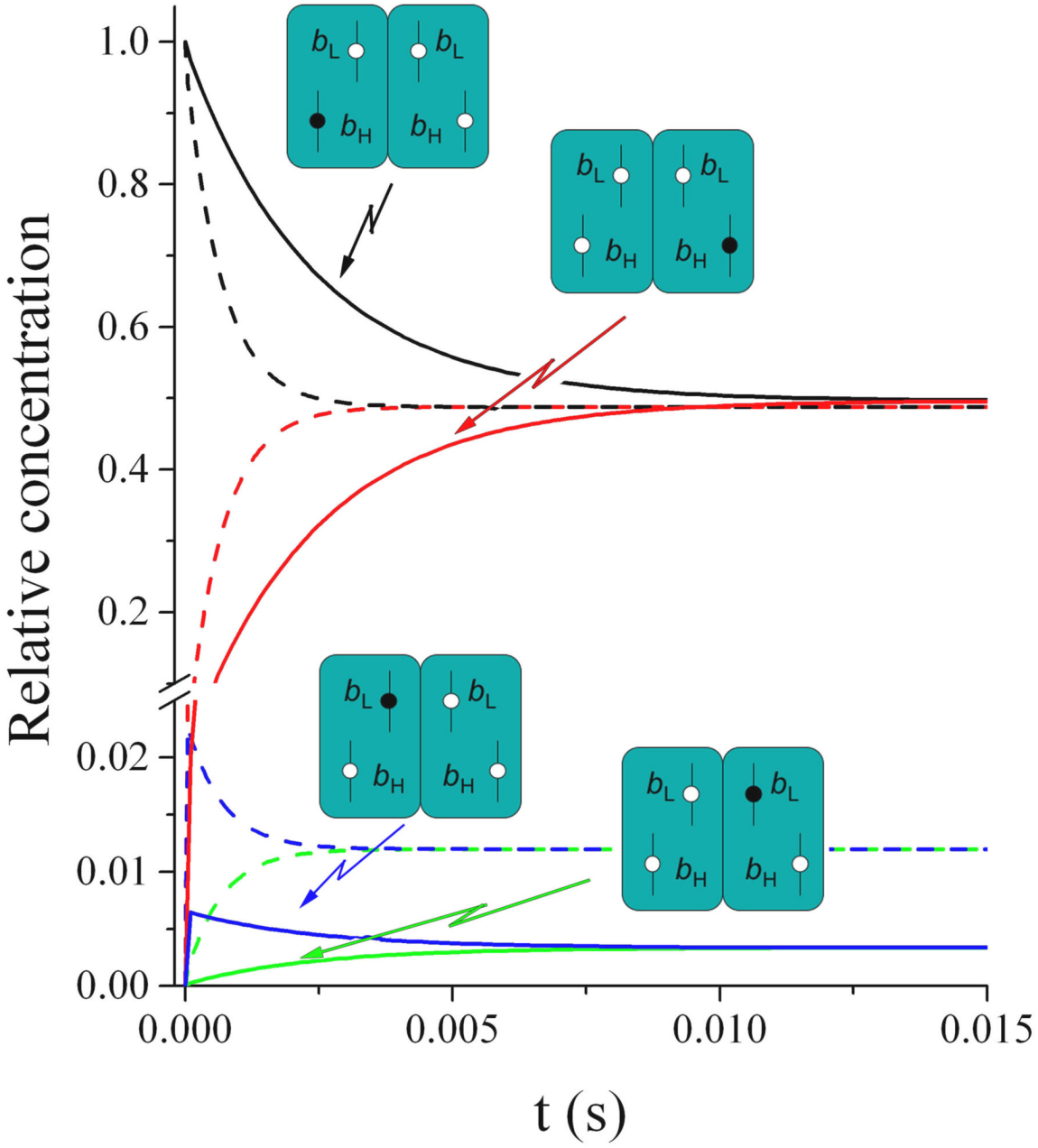

Fig. 9. Simulation of electron equilibration between the *b* hemes of the bc_1 complex dimer

Electron transfer rates between hemes were calculated using the equations in Refs. 56 & 59 (solid curves) or in Ref. 60 (dashed curves) to estimate the kinetics of electron equilibration starting from the condition in which an electron resides in one b_H heme. Changes in the relative concentration of dimers with the electron in the initial b_H heme (black curves), in the b_L heme of that same monomer (blue curves), in the opposite b_L heme (green curves), or in the opposite b_H heme (red curves) are shown. Details of the simulation program and the script file can be found in Ref. 45.

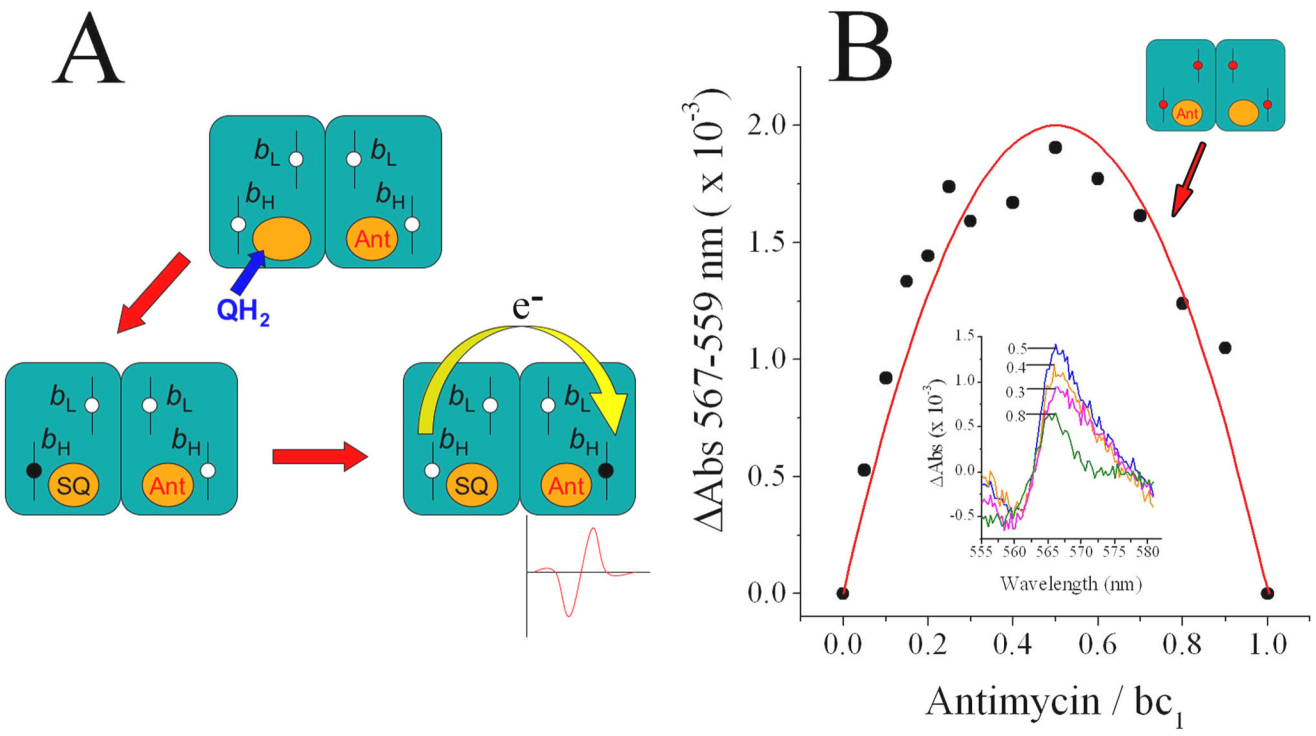

Fig. 10. Reduction of the b_H heme in antimycin-inhibited center N sites by inter-monomeric electron transfer

As shown in panel A, when both center P sites in a dimer are blocked, reduction of the b_H heme at a center N where antimycin (Ant) has been bound before addition of quinol (QH_2) can only take place if an electron is transferred from the uninhibited center N in the other monomer (yellow curved arrow). The arrival of the electron to the b_H heme in the inhibited monomer can be detected by the spectral shift induced by the bound antimycin molecule. As shown in panel B, this expected spectral shift does occur (insert) with a relative magnitude (black data points) at different antimycin/enzyme ratios that follows the predicted relative concentration of dimers with only one antimycin at center N (shown by the red curve). Experimental conditions were the same as in Fig. 2A. Data reproduced from Ref. 45.

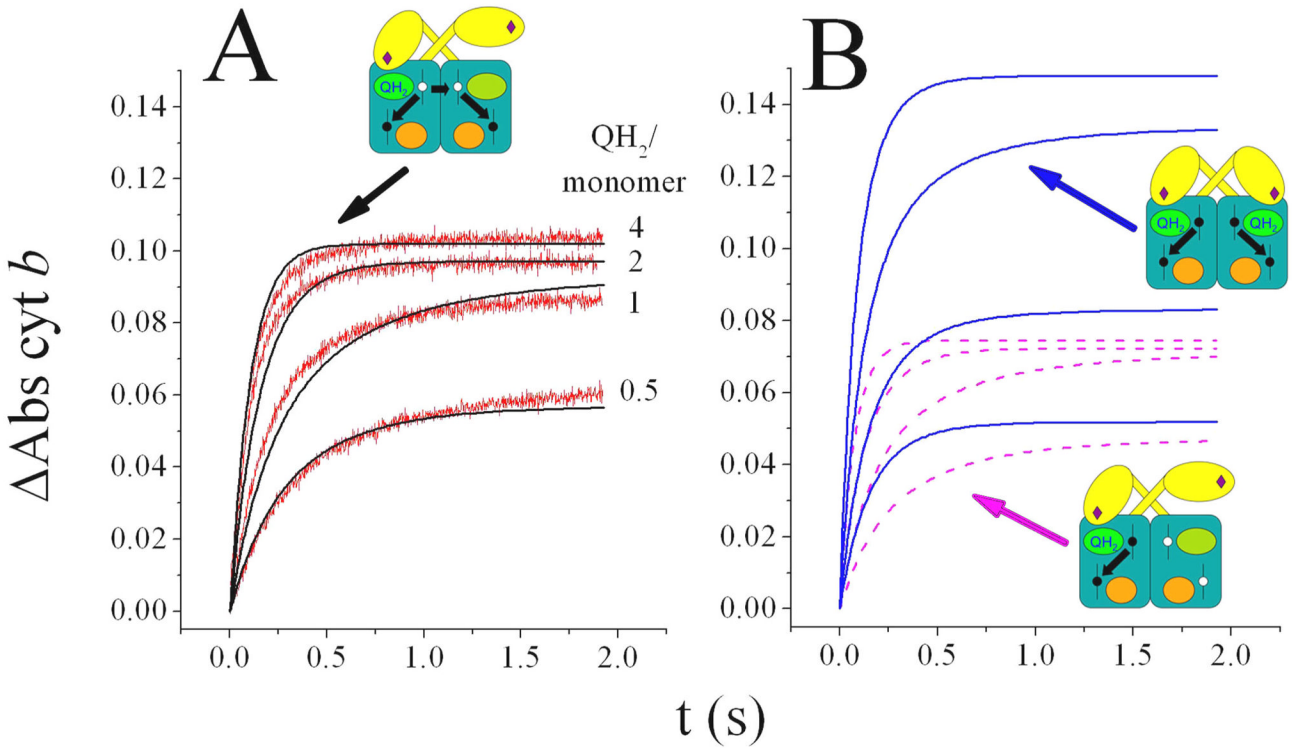

Fig. 11. Cytochrome *b* reduction kinetics in the presence of antimycin

In panel A, 1.5 μM yeast bc_1 complex reduced by the indicated quinol (QH_2) equivalents yielded cytochrome *b* reduction traces (red traces) that were simulated closely by assuming that one center P is able to reduce both b_H hemes in the dimer by inter-monomeric electron transfer (black curves). Panel B shows the simulated extents of cytochrome *b* reduction assuming catalysis at one center P without inter-monomeric electron transfer (dashed magenta curves) or assuming catalysis at both center P sites (solid blue curves). Data and simulations are from Ref. 15.

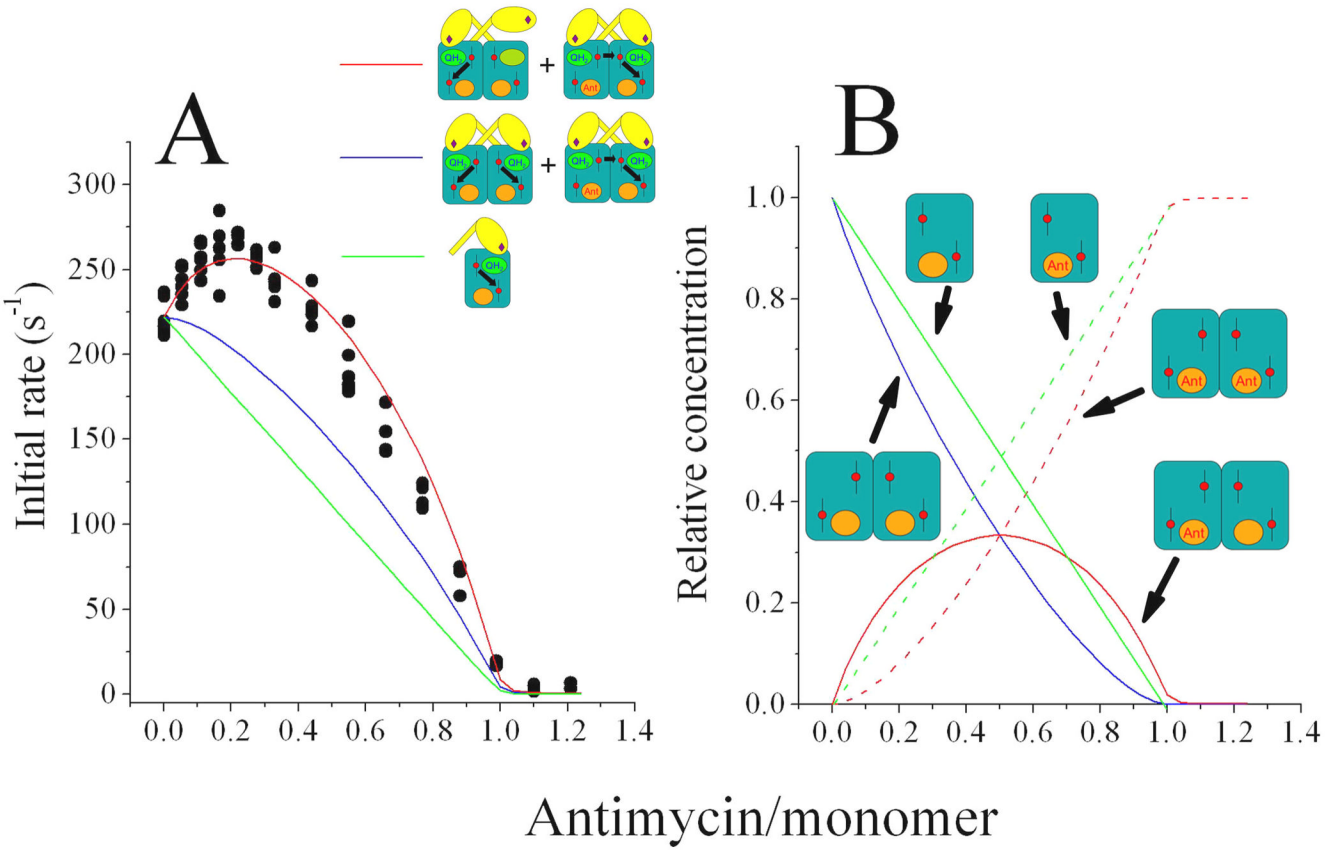

Fig. 12. Inhibition of the steady state ubiquinol-cytochrome *c* reductase activity of the yeast bc_1 complex by antimycin

Panel A shows data points (black circles) from four separate experiments in which the activity of 50 nM yeast bc_1 complex was determined in the presence of various amounts of antimycin. The change in the activity as antimycin is added can be explained by assuming that only one monomer is active in the absence of inhibitor and that both monomers become active when only one center N is blocked (simulated by the red curve). Assuming that both monomers are active in the absence of antimycin and with one inhibitor per dimer (simulated by the blue curve) does not explain the experimental data, nor does the assumption that each monomer that binds antimycin becomes inactive (simulated by the green curve). Panel B shows the relative concentrations of free and inhibitor-complexed monomers and dimers as a function of antimycin concentration from which the curves in panel A were obtained: free monomers (green solid line), antimycin-bound monomers (green dashed line), unbound dimers (blue curve), dimers with one inhibitor (red solid curve) and dimers with two inhibitors (red dashed line). Data and simulations are from Ref. 15.

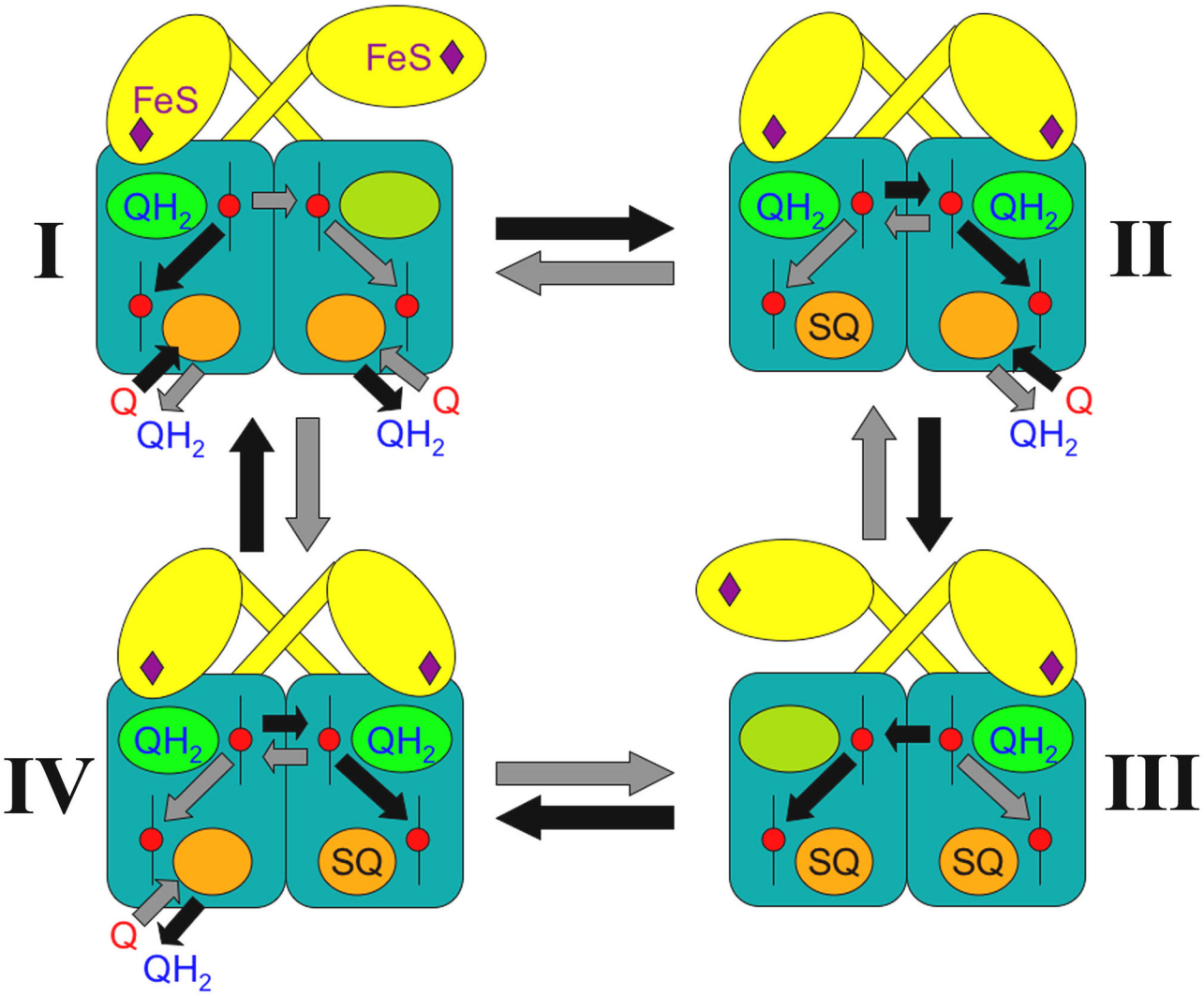

Fig. 13. Model of regulation of quinol oxidation in the dimeric cytochrome bc_1 complex

Cytochrome *b* subunits are shown as blue rectangles with potentially active center P sites as green ovals occupied by quinol (QH_2) with the Rieske protein extrinsic domain (yellow) proximal to cytochrome *b*. Center N sites are indicated by orange ovals where quinol (QH_2) or quinone (Q) bind to form semiquinone (SQ). Black and gray arrows within dimers represent possible electron transfer steps between hemes (red circles) that result in a corresponding conversion (black or gray arrows between dimers) between intermediates. See text and Ref. 36 for a detailed description of the model.